Freight From Space: Evaluating Freight Activity and Emissions from Satellite Data

CFIRE

CFIRE 04-20 June 2013

National Center for Freight & Infrastructure Research & Education
Department of Civil and Environmental Engineering
College of Engineering
University of Wisconsin–Madison

NELSON INSTITUTE
SAGE Center for Sustainability and the Global Environment
UNIVERSITY OF WISCONSIN–MADISON

Authors:
Erica Bickford and Tracey Holloway
Center for Sustainability and the Global Environment
Gaylord Nelson Institute for Environmental Studies
University of Wisconsin–Madison

Principal Investigator:
Tracey Holloway
Nelson Institute Center for Sustainability and the Global Environment
University of Wisconsin–Madison

Technical Report Documentation

1. Report No. **CFIRE 04-20**	2. Government Accession No.	3. Recipient's Catalog No.	
4. Title and Subtitle **Freight From Space: Evaluating Freight Activity and Emissions from Satellite Data**		5. Report Date **June, 2013** 6. Performing Organization Code	
7. Author/s Erica Bickford and Tracey Holloway		8. Performing Organization Report No. **CFIRE 04-20**	
9. Performing Organization Name and Address National Center for Freight and Infrastructure Research and Education (CFIRE) University of Wisconsin-Madison 1415 Engineering Drive, 2205 EH Madison, WI 53706		10. Work Unit No. (TRAIS) 11. Contract or Grant No. DTRT06-G-0020	
12. Sponsoring Organization Name and Address Research and Innovative Technology Administration U.S. Department of Transportation 1200 New Jersey Avenue, SE Washington, DC 20590		13. Type of Report and Period Covered **Final Report** **(9/1/2010 – 6/30/2013)** 14. Sponsoring Agency Code	
15. Supplementary Notes **Project completed for USDOT's RITA by CFIRE.**			
16. Abstract In this report, we investigate the current state of knowledge of freight transport emissions, the importance of freight emissions relative to other sources, and what tools are available, or can be developed to answer these questions and improve the state of knowledge on freight transportation and air quality. We build an updated version of a bottom-up roadway-by-roadway freight truck inventory (WIFE2.0) appropriate for conducting detailed, policy-relevant emissions and air quality analysis. We also employ a new freight rail inventory developed by the Eastern Regional Technical Advisory Committee. We evaluate the spatial and seasonal performance of the WIFE2.0 inventory modeled in a regional photochemical model (CMAQ) against an existing on-road diesel emissions inventory from the Lake Michigan Air Directors Consortium (LADCO), against surface observations of nitrogen dioxide (NO_2) concentrations, and against satellite retrievals of tropospheric column NO_2 from the Ozone Monitoring Instrument (OMI). Evaluation of the modeled WIFE2.0 inventory against satellite retrievals of NO_2 from OMI, compared to performance LADCO's diesel inventory, showed better spatial agreement between WIFE and OMI, however with larger bias and error, especially in urban areas. Further analysis also examined the relative contribution of freight trucks and trains to modeled surface concentrations of NO_2 in a western U.S. case study. This preliminary analysis highlights the utility of satellite data for both model validation and constraining emissions sources, especially in concert with ground-based monitors, with which surface and atmospheric column model performance can be compared. The wealth of data available from models, satellites, and monitors opens up a wide range of possible analysis directions for future work.			
17. Key Words Freight, air quality, emissions, modal shift, environment, sustainability, infrastructure, diesel pollution, truck, rail, greenhouse gases, carbon dioxide	18. Distribution Statement **No restrictions. This report is available through the Transportation Research Information Services of the National Transportation Library.**		
19. Security Classification (of this report) **Unclassified**	20. Security Classification (of this page) **Unclassified**	21. No. Of Pages 53	22. Price **-0-**

DISCLAIMER

This research was funded by the National Center for Freight and Infrastructure Research and Education. The contents of this report reflect the views of the authors, who are responsible for the facts and the accuracy of the information presented herein. This document is disseminated under the sponsorship of the Department of Transportation, University Transportation Centers Program, in the interest of information exchange. The U.S. Government assumes no liability for the contents or use thereof. The contents do not necessarily reflect the official views of the National Center for Freight and Infrastructure Research and Education, the University of Wisconsin, the Wisconsin Department of Transportation, or the USDOT's RITA at the time of publication.

Table of Contents

Tables

Figures

Executive Summary

U.S. transportation is the largest source of national nitrogen oxide (NO_x) emissions and the third largest source of fine particulate emissions ($PM_{2.5}$) - pollutants that are harmful to human health. Within the transportation sector, diesel freight transport (trucks + trains) are responsible for 20% of all U.S. NO_x and 3% of $PM_{2.5}$ emissions. Though not the largest source of anthropogenic emissions, unlike other transportation sources, domestic freight is projected to double over the next several decades, reaching 30 billion tons by 2050. The air quality impacts from increased activity, the trade-offs between activity and mandated vehicle emissions technology improvements, as well as where to make infrastructure investments that encourage sustainable freight growth, are important questions for transportation and air quality managers.

In this report, we investigate the current state of knowledge of freight transport emissions, the importance of freight emissions relative to other sources, and what tools are available, or can be developed to answer these questions and improve the state of knowledge on freight transportation and air quality. To address these research questions, we build an updated version of a bottom-up roadway-by-roadway freight truck inventory (WFE2.0) appropriate for conducting detailed, policy-relevant emissions and air quality analysis. We also employ a new freight rail inventory developed by the Eastern Regional Technical Advisory Committee. We evaluate the spatial and seasonal performance of the WFE2.0 inventory modeled in a regional photochemical model (CMAQ) against an existing on-road diesel emissions inventory from the Lake Michigan Air Directors Consortium (LADCO), against surface observations of nitrogen dioxide (NO_2) concentrations, and against satellite retrievals of total column NO_2 from the Ozone Monitoring Instrument (OMI). In this analysis, we also quantify the relationship between surface and tropospheric NO_2 concentrations, and examine relative contributions of co-located freight and passenger transportation emissions sources.

Evaluation of the modeled WFE2.0 inventory against satellite retrievals of NO_2 from OMI, compared to performance of LADCO's diesel inventory, showed better spatial agreement between WFE2.0 and OMI, however with larger bias and error, especially in urban areas. Analyses examining the relative contribution of freight trucks and trains to modeled surface concentrations of NO_2 in a western U.S. case study demonstrated that outside of urban centers, a significant percent of NO_2 pollution is attributable to diesel trucks and trains, while both gasoline vehicles and diesel trucks dominate in cities during summer. Overall, this preliminary analysis highlights the utility of satellite data for both model validation and constraining emissions sources, especially in concert with ground-based monitors, with which surface and atmospheric column model performance can be compared. The wealth of data available from models, satellites, and monitors opens up a wide range of possible analysis directions for future work.

1. Introduction

1.1 U.S. Air Quality and Freight Emissions

U.S. transportation is the largest source of national nitrogen oxide ($NO_x = NO_2 + NO$) emissions at 61%, and the third largest source (second largest anthropogenic source) of fine particulate matter ($PM_{2.5}$) at 12%. Nitrogen dioxide (NO_2) is a primary air pollutant responsible for airway inflammation and increased asthma symptoms [1]. Nitrogen oxides can react chemically in the atmosphere with ammonia and other compounds to form small particulates that are components of secondary $PM_{2.5}$. When combined with volatile organic compounds (VOCs) in the presence of sunlight, NO_x also contributes to ground-level ozone (O_3) production. Ground-level O_3 affects human health by causing or exacerbating respiratory conditions [2]. Ozone is a particularly difficult pollutant to reduce both because it is formed chemically in the atmosphere through non-linear relationships between NO_x and VOCs, and because its formation is strongly affected by topography and weather conditions. Warm summers, for example, produce more O_3 than cool summers [3], [4]. This means that reducing O_3 could require even more stringent emissions controls under a warmer future climate where production is enhanced by higher temperatures [5], [6].

Within the transportation sector, Heavy Duty Diesel Vehicles (HDDVs) are responsible for 24% of transportation NO_x emissions and 15% of all NO_x emissions [7]. These HDDVs are buses, garbage trucks, and municipal vehicles, but mostly, they are freight trucks. Although diesel freight trucks are not the largest pollutant source sector, it is a sector expected to grow rapidly in the coming decades as globalization and international trade are predicted to double U.S. domestic freight tonnage to 30 billion tons by 2050 [8]. Increased freight tonnage will expand vehicle activity at urban ports and potentially double the number of trucks on the road.

Figure 1.1.1 illustrates the growth of freight truck and passenger vehicle miles traveled (VMT) relative to base year 1999. In the figure, which shows relative growth, the impacts of the recent economic slow-down are readily apparent, with a freight truck VMT peak in 2008 followed by a few years of decline before activity is projected to pick up again starting in 2013. The U.S Energy Information Administration's Annual Energy Outlook 2012 projects that between 2010 and 2035, the rate for freight truck VMT growth will be 1.6% compared to 1.2% for passenger VMT [9]. This activity growth, occurring simultaneously with increasingly stringent air pollution standards, means the freight sector could play a much larger role in future U.S. emissions. This role is complicated by the shift toward "just in time" delivery structures where manufacturers and retailers reduce costs associated with on-site inventory storage in favor of more frequent deliveries, the transition of new freight trucks and freight trains transition to ultra-low sulfur diesel (ULSD), the exploration of natural gas as an alternative fuel, and pressure to adhere to more stringent NO_x and $PM_{2.5}$ emissions standards. This trade-off

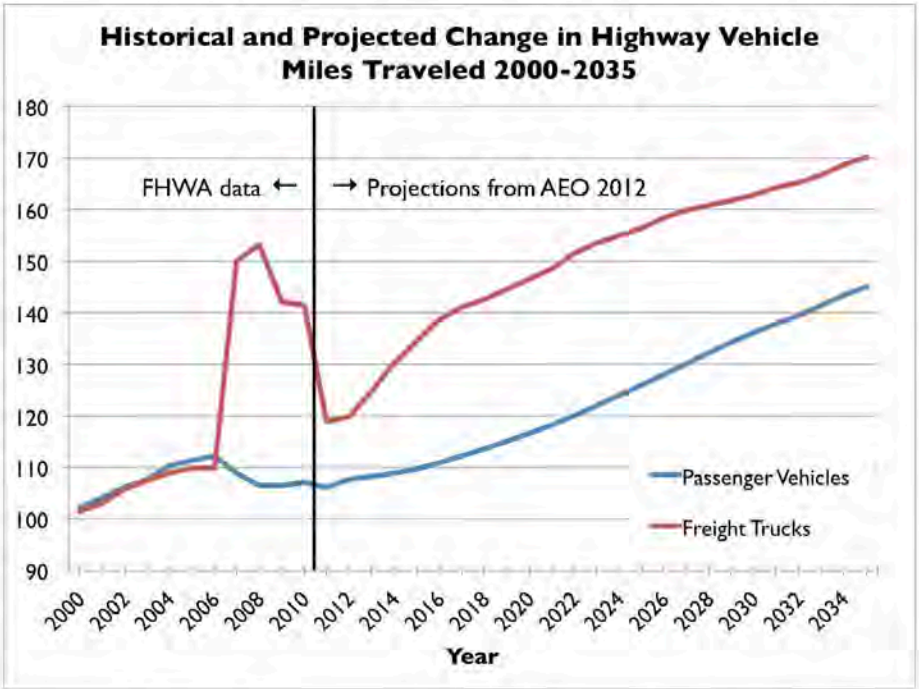

Figure 1.1.1 *Historical and projected changes in vehicle miles traveled (VMT) for passenger vehicles and freight trucks relative to 1999 VMT. Data for 1999 to 2010 was taken from FHWA's Highway Statistics publications for 1999 to 2010, table VM-1. Projections for future VMT (2011 to 2035) were taken from the 2012 Annual Energy Outlook (AEO) table of Transportation Sector Key Indicators.*

introduces some uncertainty as to what the emissions balance will be between emissions technology improvements and activity growth. In addition to emissions, a doubling of freight activity also means investments will have to be made to handle vehicle activity. How infrastructure investments are made, and to what extent they preferentially consider mode sustainability, could also have significant air quality impacts, both directly, and indirectly through affecting passenger vehicle congestion.

Here we investigate the current state of knowledge of freight transport emissions, the importance of freight emissions relative to other sources, and what tools are available, or can be developed to answer these questions and improve the state of knowledge of freight transportation and air quality.

1.2 Satellite Data for Air Quality Analysis

Since 1995, 42 instruments related to air quality measurements have been put into orbit onboard satellites [10]. In recent years, researchers have used satellite air quality data to analyze spatial and temporal emissions trends of anthropogenic and natural activity both on land, and over the ocean. With satellite observations of NO_2, several studies

have tracked multi-year trends in global anthropogenic emissions patterns, from increases associated with a rapidly industrializing China, to decreases related to environmental regulations and economic slowdown. Using satellite observations of NO_2 from the Global Ozone Monitoring Experiment (GOME) and the SCanning Imaging Absorption spectroMeter for Atmospheric CartograpHy (SCIAMACHY) from 1996-2006, van der A et al. [11] observed -7% emissions reductions in Europe and parts of the eastern U.S., with up to +29% increases in China over the same period. Kim et al. [12], using GOME, similarly found up to -38% decreases from 1999-2005 in NO_2 concentrations along the Ohio River Valley, attributed to environmental regulations requiring improved power plant pollutant controls. Russell et al. [13] examined weekly cycles and multi-year trends of NO_2 in California from 2005-2008 using data from the Ozone Monitoring Instrument (OMI), observing a -9% decrease in emissions from Los Angeles over the period as well as a consistently strong weekday/weekend cycle they speculated was the result of lower HDDV activity on weekends.

Due to limited confounding and background emissions sources, shipping emissions across oceans and seas have been a focus area for satellite analysis of anthropogenic emissions. Richter et al. [14] analyzed tropospheric NO_2 signatures from SCIAMACHY in the Indian Ocean, finding clear patterns of ship tracts visible from satellite retrievals that compared well with ship inventory spatial distributions. Marbach [15] conversely used formaldehyde measurements from GOME to examine ship tracts over the Indian Ocean and compare against model estimates, finding modeled concentrations to be two times lower than satellite retrievals. Marmer et al. [16] used OMI NO_2 to validate three separate ship emissions inventories for the Mediterranean Sea, concluding all inventories over-estimated ship NO_2 emissions. Franke et al. [17] investigated the application of satellite NO_2 retrievals from SCIAMACHY, GOME and GOME-2 for shipping inventory validation of the lane from India to Indonesia, finding good agreement between modeled inventory emissions and satellite retrievals. Finally, de Ruyter de Wildt et al. [18] used satellite retrievals of NO_2 from SCIAMACHY, GOME, OMI and GOME-2 to observe global trends in economic activity, identifying a 62% to 109% increase in shipping between 2003 and 2008, and 12% - 36% decline after 2008.

Yet while these and many other studies have effectively employed satellite observed pollutant concentrations to evaluate industrial activity and pollutant chemistry, few studies to date have used satellite data to evaluate surface transportation emissions, and none have used satellite data to validate surface freight transportation inventories. Surface freight transportation is comprised of trucks and rail, which together move 91% of domestic freight tonnage (73% for trucks and 18% for rail), with the remaining 9% carried by airplanes and barges [8]. Diesel freight trucks and trains are significant sources of air pollution. Combined, they are responsible for 32% of transportation nitrogen oxide emissions, 21% of transportation $PM_{2.5}$ emissions and 36% of transportation carbon dioxide (CO_2) emissions [7], [9], [19]. Lack of publicly available freight rail activity and fleet data has impeded efforts to create detailed rail emissions

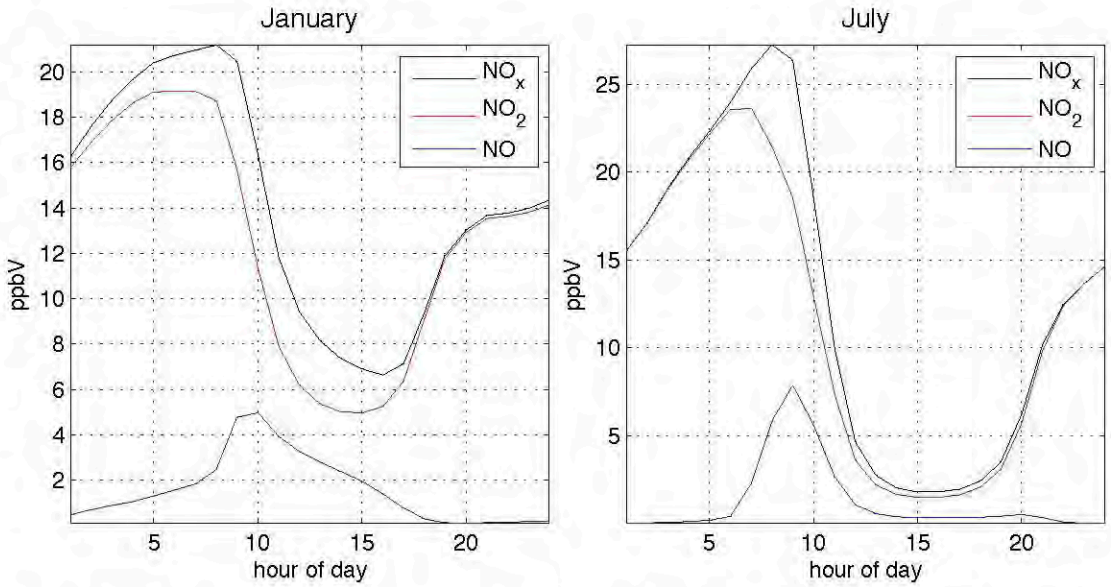

Figure 1.2.1 *CMAQ modeled monthly mean diurnal concentration pattern for NO, NO_2 and NO_x over Madison, WI in January and July 2007. Concentrations of NO peak early in the day before dropping off at night when NO is converted to NO_2. Concentrations of NO_2 track closely with concentrations of NO_x.*

inventories with timely updates. Truck freight activity patterns differ from passenger vehicle patterns, often operating in high densities on rural interstates. The mobile nature of these emitters, various engine types, vehicle ages and payloads, make it difficult to spatially and temporally quantify their emissions.

The U.S. maintains a network of surface pollutant monitors (see Figure I.i in Appendix I), for the purpose of monitoring air quality to protect human health. Most surface monitors are concentrated in urban regions, with little or no coverage in rural areas where both freight truck and rail extensively operate. Thus, their utility for evaluating spatially expansive emissions sources like highway and railway networks is limited. Freight vehicles traverse the continental U.S., operating on over 450,000 miles of highway and over 100,000 miles of railroad track. To improve estimates of surface freight transportation emissions, focusing on diesel trucks and locomotives, we employ satellite data, with near complete spatial coverage of the U.S., to inform and evaluate performance of our bottom-up Wisconsin Inventory of Freight Emissions (WIFE). In this analysis, retrievals of NO_2 from OMI for 2007 are used to evaluate our diesel freight truck emissions inventory modeled in CMAQ. Though for air quality NO_2 and NO are usually considered together as NO_x, currently there are no satellite products that retrieve NO (or many other transportation relevant pollutants at the temporal and spatial scales necessary for this analysis). Therefore, only NO_2 is considered in this report. Figure 1.2.1 illustrates the relationship between concentrations of the ozone precursor, NO_x with concentrations of NO_2 and NO; clearly concentrations of NO_2 track closely with concentration trends of NO_x. In this analysis, we also quantify the relationship between

surface and tropospheric NO_2 concentrations, and examine relative contributions of co-located freight and passenger transportation emissions sources.

2. Data and Methods

2.1 WIFE2.0

In this analysis, we used the same fundamental methodology employed to develop earlier versions of the WIFE inventory described in Johnston et al. [20] and CFIRE report 02-09: *Sustainable Freight Infrastructure to Meet Climate and Air Quality Goals* [21]. However, here we employ the newer Freight Analysis Framework version 3.0 (FAF3) [22] with base year 2007 activity, and the EPA's new MOtor Vehicle Emissions Simulator (MOVES) [23], [24] model to generate running exhaust emissions factors as well as idling and coldstart emissions totals. The motivation for generating our own diesel freight inventory is both to serve the freight analysis community by answering questions specifically related to freight transport activities and examine the magnitudes and spatial extent of this sector's contribution to pollutant emissions. We include non-freight emissions inventory data for power plants, gasoline vehicles, off-road vehicles, industry, biogenic and natural sources from the Lake Michigan Air Directors Consortium's (LADCO) 2007 emissions inventory. The LADCO inventory groups all diesel motor vehicle emissions together. In order to swap in our WIFE inventory and not under-represent vehicle emissions by excluding non-freight diesel vehicles, in this version of WIFE we also account for non-freight highway diesel emissions using traffic activity fields in FAF3. We call this version of the inventory, WIFE2.0.

The FAF3 activity database links to a GIS roadway shapefile, where each roadway link is associated with activity fields for 2007 average annual daily traffic (AADT07), 2007 average annual daily long-haul freight truck traffic (FAF07), and 2007 average annual daily non long-haul freight traffic (NONFAF07). These activity estimates were derived for FAF3 from a combination of the 2008 Highway Performance Monitoring System (HPMS) database, state truck percentage, and origin-destination freight truck transport modeling. To estimate non-freight diesel highway activity, we took the difference between AADT07 and all freight traffic (All Freight Traffic = FAF07 + NONFAF07). Non-freight vehicle activity was allocated to passenger cars, buses, and other 2 axle-4 tire vehicles using standard vehicle miles traveled (VMT) distributions for vehicle class and road type in MOVES documentation [24], [25].

While earlier versions of FAF excluded empty truck trips, in FAF3, empty movements were included in activity estimates, and therefore empty trucks in WIFE2.0 did not need to be estimated and added back in. However, in WIFE2.0, we are still quantifying diesel vehicle emissions only, so we did need to estimate the percent of diesel vehicles in each vehicle activity category. For earlier versions of WIFE, we assumed diesel freight

trucks accounted for 98% of freight VMT [21]. However, MOVES has different vehicle categories than the EPA's previous MOBILE6.2 vehicle emissions model, so we adjusted our freight diesel vehicle estimates, and expanded them to non-freight vehicles as well. Diesel VMT fractions by vehicle type and MOVES road type were estimated using MOVES documentation for VMT distribution, and diesel fractions [24], [25]. Table 2.1.1 shows vehicle fleet diesel percentages (not VMT percentages) used in this analysis. Table 2.1.2 shows the methodological break-down between earlier versions of the WIFE inventory and WIFE2.0.

Vehicle Diesel Fractions	
Single-Unit Freight Trucks	70%
Combination Unit Freight Trucks	100%
Passenger Cars	0.38%
Buses	93%
Other 2 axle-4 tire Vehicles	3.46%

Table 2.1.1 *Vehicle diesel fractions. Other 2 axle-4 tire vehicles include SUVs, minivans and light trucks.*

On recommendation from MOVES developers at EPA (personal communication with Chris Dresser, February, 2012) we generated running exhaust emissions factors for two counties to represent the two diesel fuel regimes in the U.S. in 2007. Diesel vehicle emissions factors in MOVES change geographically only based on fuel properties (personal communication with Chris Dresser, February, 2012). In 2007, California diesel fuel had an average fuel sulfur level of 11 ppm and the rest of the U.S. diesel fuel had an average fuel sulfur content of 43 ppm [24]. To represent California and the rest of the country, we selected representative counties in the center of each domain. Fresno county in California, and Ellis county in Kansas for the remainder of the U.S. Emissions factors were generated for all diesel vehicles on all road types, for all CMAQ pollutants, for running exhaust, crankcase running exhaust, and tire and brake wear. Unlike MOBILE6.2, MOVES automatically calculates emissions factors for 16 speed bins from 2.5 mph to 75 mph. Curves were fit to emissions factors as a function of speed. While earlier emissions factors calculated by MOBILE6.2 best fit a quadratic curve, emissions factors by MOVES best fit a power curve (see Figure II.i in Appendix II). Power curves

Inventory Methods	WIFE	WIFE2.0
Years	2002, 2005, 2009, 2018	2007
Activity Data	FAF2	FAF3
Activity Data Includes Empty Freight Movements?	No	Yes
Emissions Factors	MOBILE6.2	MOVES
Idling and Cold Start Emissions?	No	Yes
Weekday/Weekend Accounting	No	Yes (for idling and cold starts)
Non-Freight Diesel Vehicles?	No	Yes

Table 2.1.2 *Inventory methodology break-down between earlier versions of WIFE and WIFE2.0*

were generated for two counties, for two months, for seven vehicle classes, for four road types, for sixteen pollutants, resulting in 1,792 emissions factor speed curves. Upon analyzing the speed curves, it was discovered that although MOVES has four road types, two of the road types fall under the "arterial" roadway classification, and two fall under the "freeway" roadway classification - effectively resulting in diesel emissions factors for only two road types. Further, once emission factor power curves were generated for each of these two road types, it was found that the curves were very similar, with diesel emissions varying much more with speed than with road type. To minimize the computational intensity of applying emissions factor speed curves to activity data in FAF3, we averaged diesel emissions factors across road types, leaving 448 equations for emissions factor curves to be applied to the activity data.

Emissions factor speed curves were applied to freight and non-freight VMT and road segments in the FAF3 activity-linked roadway shapefile as a function of roadway speeds included in FAF3, according to equation 2.1.1:

Equation 2.1.1 $\text{Emissions(grams)} = \text{VMT(miles)} \times (C \times S^b) \times \text{pollutant(grams/mile)}$

Where VMT is for a given vehicle class on a given roadway segment, S is the field "SPEED07" in FAF3 that is the peak period speed for that roadway segment, and C and b represent the power curve coefficients for a given pollutant, vehicle class, month and geographic region. Separate inventories for freight and non-freight diesel vehicle emissions were built from the FAF3 activity database and shapefile. These inventories were gridded to a 36 km x 36 km continental U.S. model grid to match the LADCO national inventory model grid, and a 12 km x 12 km upper Midwest grid to match LADCO's midwest model grid.

For HDDVs, running exhaust emissions do not capture the total emissions associated with diesel vehicles. Idling and cold start emissions can be a substantial source of emissions, especially for NO_x [26], [27]. To include idling and cold start diesel emissions in WIFE2.0, we again used MOVES. However, MOVES cannot generate emissions factors for idling and cold starts because calculations for those emissions are based on vehicle population data linked to counties. Therefore, we used MOVES to generate a 2007 diesel idling and cold start county-level emissions inventory. County-level emissions were interpolated using area weighting to the LADCO 36 km x 36 km national grid, and 12 km x 12 km Midwest grid. Because the majority of idling and cold start diesel emissions are associated with HDDV freight vehicles, all idling emissions were combined with the freight running exhaust inventory, and no idling emissions were included in the non-freight diesel inventory.

For inventory generation, MOVES has the capacity to create separate inventories for weekdays and weekends. Because FAF3 activity data only include average annual activity, running exhaust emissions inventories do not exhibit diurnal or weekly

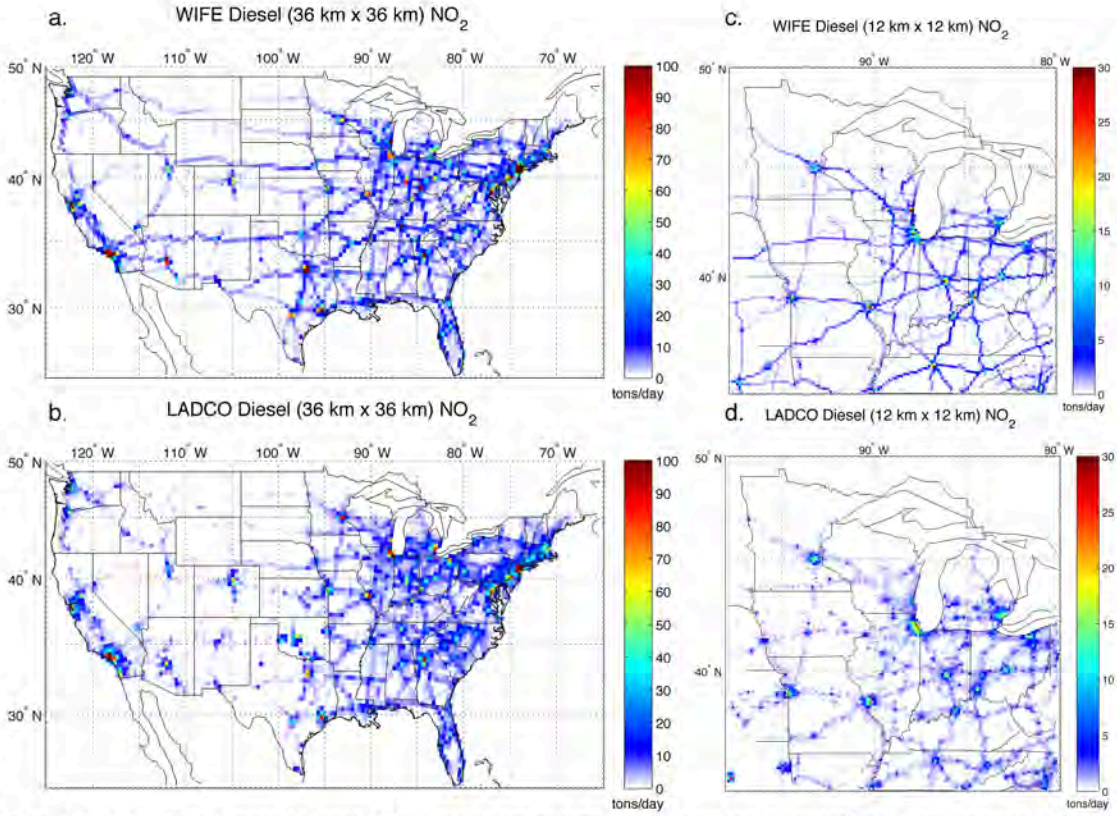

Figure 2.1.1 *2007 January diesel NO_2 emissions inventory comparison (in tons/day) between the WIFE freight + non-freight on-road diesel inventory and LADCO's on-road diesel inventory, for the continental U.S. gridded to 36 x 36 km², and the upper Midwest gridded to 12 x 12 km².*

emissions patterns. To improve representation of temporal freight emissions patterns, average daily running exhaust emissions were combined with weekday idling emissions, and weekend idling emissions to create representative weekday and weekend diesel freight emissions inventories. The final result was three representative diesel inventories for each month (January and July), 1) weekday diesel truck freight inventory, 2) weekend diesel truck freight inventory and 3) average day non-freight diesel inventory. All inventories were speciated for air quality modeling using speciation tables for diesel vehicles from the Sparse Matrix Operator Kernel Emissions (SMOKE) model [28]. Methods for inventory speciation followed those described in detail in Bickford [21], using updated speciation tables for the Carbon Bond 5-CI (CB05-CI) chemical mechanism.

The WIFE2.0 diesel inventories were compared against LADCO's on-road diesel inventories as a check against errors or inconsistencies. Figure 2.1.1 shows January 2007 weekday diesel emissions (tons/day) of NO_2 for both the WIFE2.0 (freight + nonfreight) and LADCO inventories, at both grid resolutions. Evident in the figure is how the bottom-up, shapefile based WIFE inventory retains more highway network structure

than LADCO's, particularly at the 12 km Midwest grid resolution. Rural emissions magnitudes compare well between WIFE2.0 and LADCO, while WIFE2.0 exhibits generally higher urban emissions with the notable exception of Chicago. Overall, NO_2 emissions in the 36 km x 36 km WIFE2.0 inventory are 4.8% higher than LADCO in January, and 16.7% lower in July, while in the 12 km x 12 km inventory, NO_2 in WIFE2.0 is 6.5% lower in January, and 25.7% lower in July.

2.2 Updated Rail Inventory

Another improvement to the representation of freight emissions in this analysis is the utilization of a new bottom-up freight rail emissions inventory from the Eastern Regional Technical Advisory Committee (ERTAC) [29]. Earlier rail freight inventories lacked the spatial resolution and timely updating necessary for air quality modeling. Inventory methodologies varied widely from state to state, and little if any detailed data on locomotive fleet sizes, operating geography or activity levels that could help improve inventory estimates was publicly available. Through ERTAC, air protection agencies from 27 states coordinated to build a cohesive, nationwide railroad emissions inventory for 2007/2008 based on local operations, with data and support from the rail industry.

The ERTAC inventory was obtained from LADCO as GIS shapefiles with associated emissions databases. The inventory was gridded to LADCO's 36 km x 36 km national grid, and 12 km x 12 km Midwest grid (see Appendix III for details on this methodology). Locomotive emissions factors were speciated for air quality modeling following the methodology detailed in Bickford [21], with updated SMOKE speciation tables for CB05-CI.

The ERTAC rail emissions inventory includes link-level annual emissions estimates for Class-I linehaul locomotives (large, long-haul freight carriers), Class-II/III linehaul locomotives (local and regional short-haul freight carriers), and Class-I railyard switching engines - which can be a significant source of emissions near urban populations. To generate the Class-I linehaul and railyard inventories, Class-I railroad carriers allowed ERTAC, under a confidentiality agreement, to access a link-level GIS rail activity dataset, and railyard database managed by the Federal Railroad Administration (FRA). Rail carriers also provided fleet mix information, from which ERTAC calculated weighted emissions factors based on the age distribution of their fleet, and the proportion of locomotives in each of the U.S. EPA's emissions "Tier" categories. For more detail on the development of the ERTAC rail inventories, see Bergin et al. [30]-[32].

While the ERTAC inventory represents a significant improvement in the spatial resolution of rail emissions, and representation of carrier fleets and activity, there are still some limitations. The inventory does not include seasonal accounting or diurnal distribution, and excludes passenger locomotive emissions like Amtrak. While activity for large Class-I linehaul carriers is likely to be more or less constant throughout the

year - and as the largest source of rail emissions, most relevant for air quality purposes - that may not hold true for shorthaul carriers. Irrespective of seasonal activity changes, emissions factors calculated for the ERTAC inventory are also not temperature dependent. In reality, it is likely that seasonal temperatures do have some effect on locomotive emissions factors, just as they do for HDDVs. Questions like seasonal temperature effects on locomotive emissions rates, though not addressed in this work, could possibly be examined using satellite retrievals and improve inventory development in the future.

2.3 Air Quality Modeling

To compare freight inventory estimates to satellite retrievals, we modeled atmospheric chemistry with the Community Multiscale Air Quality Model (CMAQ) version 4.7.1 [33]. Meteorological inputs were generated for CMAQ using the Weather Research and Forecasting (WRF) model version 3.0 with 2007 North American Regional Reanalysis (NARR) to simulate meteorology for December 2006, January, June and and July 2007. Hourly meteorology files output by WRF for each day were processed for CMAQ using the Meteorology-Chemistry Interface Processor (MCIP) version 3.6.

In addition to the WIFE2.0 and ERTAC diesel inventories, non-freight emissions from LADCO's 2007 36 km x 36 km national and 12 km x 12 km Midwest emissions inventories were converted from emissions files, built for use with the Comprehensive Air Quality Model with Extensions (CAMx), to CMAQ compatible file formats. All emissions files were grouped for processing in CMAQ with the merge component of the SMOKE model.

Several experimental runs were performed with CMAQ to evaluate emissions inventory performance and conduct pollution attribution analysis. Basecase model runs were performed with both WIFE2.0 and LADCO diesel inventories on both the 36 km x 36 km national, and 12 km x 12 km Midwest grids for January and July 2007. Basecase runs are used for model validation against surface observations and satellite retrievals. To quantify relative contributions of different transportation emissions sources, we also conducted CMAQ runs at 36 km x 36 km for January and July 2007 where diesel trucks were removed, where diesel trains were removed, and where gasoline vehicles were removed. The latter experiments used the WIFE2.0 diesel freight and non-freight inventories, because it allowed for selected removal of specific freight-truck diesel emissions while leaving non-freight diesel emissions in.

2.4 OMI NO_2 and Tropospheric Column NO_2 from CMAQ

Satellite retrievals of tropospheric column NO_2 from OMI [34] were obtained and processed for model comparison. OMI is a UV/Vis nadir spectrometer onboard NASA's Aura satellite. The instrument is a collaboration between NASA and the Netherlands Agency for Aerospace Programs (NIVR). OMI operates on a polar orbiting satellite with

13 km x 24 km resolution, and daily global coverage. The instrument measures ozone, NO_2, sulfur dioxide, formaldehyde, aerosols, and other compounds relevant to stratospheric and tropospheric chemistry. Data is available from October 2004 to the present. Following from Herron-Thorpe et al. [35] and Boersma et al. [36], we used the Dutch OMI NO_2 (DOMINO) level-2 data product version 2.0 from KNMI [37]. This latest version of the DOMINO product corrects errors in air mass factor calculations that resulted in high biases of 0-40% in previous versions [36], [38].

The DOMINO Level-2 product was processed with the Wisconsin Horizontal Interpolation Program for Satellites (WHIPS), developed by Jacob Oberman at the University of Wisconsin (see Holloway et al., 2012, in prep). WHIPS is a Python-based, open-source software that interpolates and averages level-2 satellite retrievals from their native latitude and longitude based grid onto a user-defined fixed grid, such as those used in air quality models. Re-gridding satellite retrievals to air quality model grids facilitates one-to-one comparisons between models and satellite data. We processed DOMINO Level-2 NO_2 from January and July 2007 onto the LADCO 36 km x 36 km national model grid, and the 12 km x 12km Midwest model grid.

To compare CMAQ model output to WHIPS processed OMI NO_2, some further processing of CMAQ output was also necessary to convert layer concentrations produced by the model to tropospheric column NO_2 retrieved by the satellite instrument. To do this, for each gridcell, and for each day, we extracted NO_2 data from CMAQ instantaneous concentration hourly output files (CCTM CONC), time-interpolated the CMAQ output to match OMI overpass time (approximately 1:30pm local time), and time-interpolated atmospheric pressure values from the model's meteorology files to match OMI overpass time. We masked the model output where satellite data were missing due to clouds or other interference, and interpolated model mid-layer pressure levels to OMI mid-layer pressure levels which were derived from the Tropospheric Model 4 (TM4) [37]. We used log-linear interpolation to estimate OMI pressure levels at layer tops from which we calculated the change in pressure over each layer. We zeroed out the OMI averaging kernel above the tropopause and scaled it for the troposphere, then we converted the CMAQ model NO_2 concentration to total column NO_2 in units of 10^{15} molecules per cm^2 [39], and finally, matrix multiplied the model by the averaging kernel to create one-to-one OMI-comparable tropospheric column NO_2.

The averaging kernel quantifies the contribution of the stratosphere, troposphere and boundary layer to the instrument observation, and is proportional to the height-dependent sensitivity of the satellite observation to changes in trace concentration [40]. The averaging kernel distributed with satellite products is required to accurately compare total column pollutant concentrations produced by models, to concentrations retrieved by satellites. Applying the averaging kernel applies the vertical layer distribution assumptions used in creating the Level-2 satellite product to the model data making OMI and CMAQ directly comparable.

3. Results

Results from the analysis are presented here, beginning with validation of surface NO_2 concentrations from CMAQ against surface observations from EPA's Air Quality System (AQS), and following with validation of tropospheric column NO_2 from CMAQ against OMI retrievals. Validation results include comparison of model performance against satellite observations in gridcells containing AQS surface monitors, and model comparison against OMI in rural areas. Finally, we examine the relationship between tropospheric column NO_2 and surface NO_2, and look at a case study of freight-related emissions in the Western U.S.

3.1 Model Validation: AQS and OMI

Figures 3.1.1 and 3.1.2 show maps of CMAQ monthly mean surface NO_2 for January and July 2007 for basecase model runs using the WIFE2.0 diesel inventory, and the LADCO diesel inventory for the 36 km x 36 km national domain. Overlaid on the maps are monthly mean measured AQS NO_2. Inventory model runs compare reasonably with model observations. Both inventory model runs are too low in urban areas in January, and are a little too high in some areas in July. In the WIFE2.0 model run, roadway structures are a little more evident across the rural Western U.S. Scatterplots in Figures 3.1.1 and 3.1.2 show the spatial agreement between monthly mean NO_2 in observations and the model, with spatial correlation values. In both months, spatial correlations of monthly means are a little higher for CMAQ runs with the WIFE2.0 inventory, giving a preliminary indication that the WIFE2.0 inventory improves on the spatial distribution of freight truck emissions over the LADCO diesel inventory.

Figures 3.1.3 and 3.1.4 show a similar comparison between 36 km x 36 km CMAQ monthly mean tropospheric column NO_2, and monthly mean OMI tropospheric column NO_2 for basecase model runs with the WIFE2.0 and LADCO diesel inventories. Compared to the largely urban, and very localized AQS observations, OMI provides concentrations on a model-comparable grid scale. Maps show the absolute difference in column NO_2 between the model and the satellite (CMAQ-OMI), while scatterplots illustrate spatial correlations. Grayed out areas on the maps indicate where satellite data was unavailable, often due to cloud cover or high surface reflectivity due to snow cover. With many more spatial points for comparison, we see from the difference maps that in January, both diesel inventory model runs are too high over the eastern half of the U.S. - particularly in the Ohio River Valley, and also high over metropolitan areas in southern California and the Bay Area, while NO_2 concentrations in parts of the Southwest, and in the Chicago area are too low. The WIFE2.0 inventory shows higher concentrations in Los Angeles, and eastern Texas compared to LADCO diesel, while showing better agreement around the Southwest and Mountain West. In July, both inventory model runs are lower than the satellite, with the exception of urban areas in California, where both models are too high. Again, the WIFE2.0 inventory model run

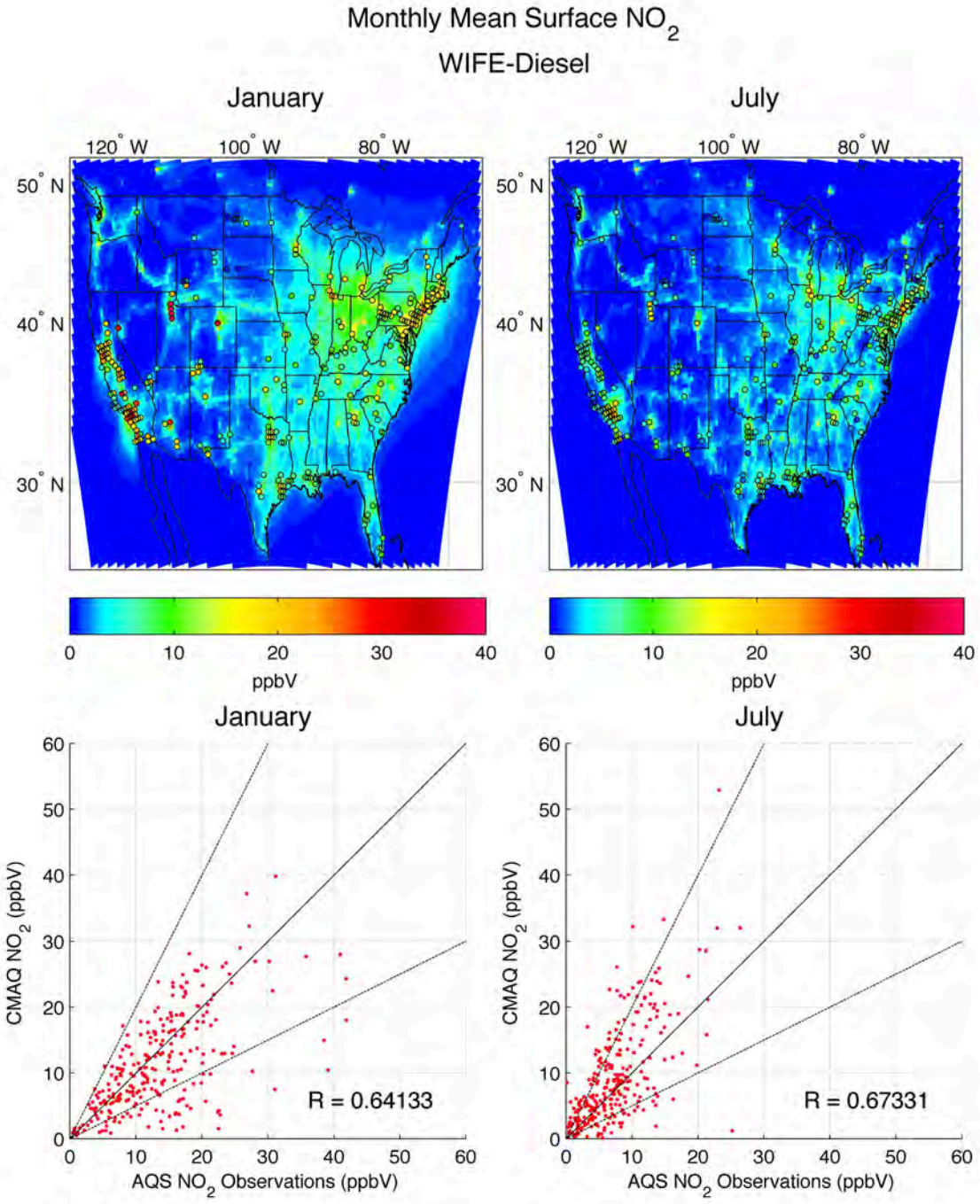

Figure 3.1.1 *CMAQ modeled 36 km x 36 km a) January and b) July 2007 monthly mean surface NO_2 using the WIFE diesel inventory, overlaid with monthly mean AQS NO_2 observations. CMAQ modeled c) January and d) July monthly mean surface NO2 (y-axis) scattered against monthly mean AQS observations (x-axis), with a 1:1 line (solid), a 2:1 line (dashed), a 1:2 line (dashed), and spatial correlation value, R.*

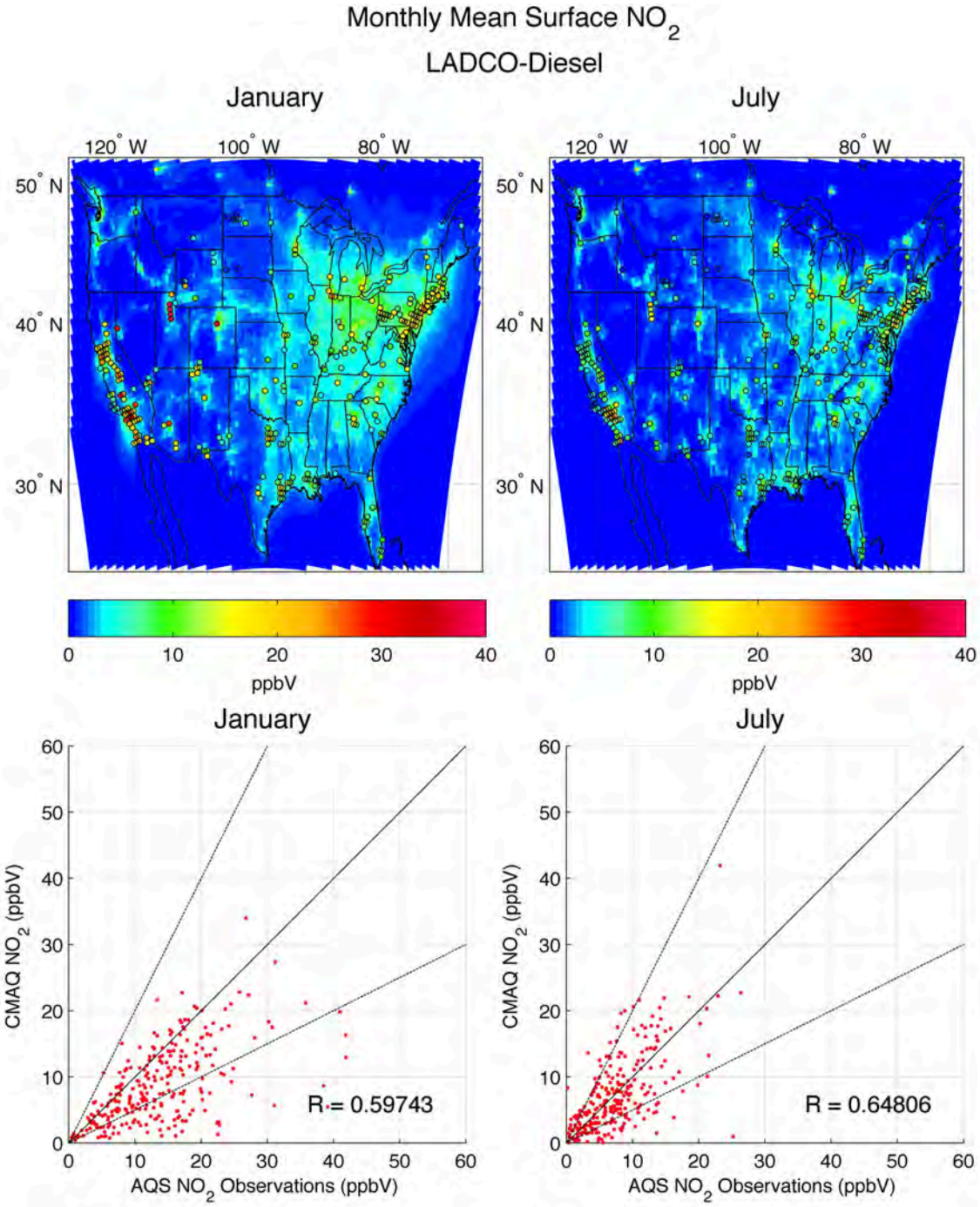

Figure 3.1.2 *CMAQ modeled 36 km x 36 km a) January and b) July 2007 monthly mean surface NO_2 using the LADCO diesel inventory, overlaid with monthly mean AQS NO2 observations. CMAQ modeled c) January and d) July monthly mean surface NO_2 (y-axis) scattered against monthly mean AQS observations (x-axis), with a 1:1 line (solid), a 2:1 line (dashed), a 1:2 line (dashed), and spatial correlation value, R.*

concentrations are more elevated than the LADCO run in Southern California. Though overall model-satellite agreement may be determined by emissions sources other than freight, spatial and concentration differences between the WIFE2.0 and LADCO OMI difference maps are attributable solely to their different estimates of surface freight emissions.

Scatterplots for the CMAQ-OMI 36 km x 36 km comparison show higher spatial correlation values than was observed with AQS validation. January scatterplots for WIFE2.0 and LADCO diesel are clustered between the 1:1 and 2:1 lines, indicating that the modeled tropospheric column NO_2 is approximately 1.5 times as high as OMI column NO_2. This result could be due either to inventory emissions estimates or model chemistry. Despite the magnitude differences, the spatial patterns in January compare quite well, with correlation values around 0.89. Interestingly, in January, the WIFE2.0 CMAQ run shows a slightly better spatial correlation (0.889 compared to 0.883), while in July, the LADCO CMAQ run has a better spatial correlation value (0.723 compared to 0.684), indicating that inventory performance in the model varies between seasons.

One of the motivations for building the WIFE2.0 inventory was that existing inventories likely over-allocate freight-truck emissions to urban areas rather than rural areas due to population weighting of activity. We were therefore interested in evaluating our inventory against satellite observations (and the LADCO diesel inventory) in rural areas to test its performance. Figure 3.1.5 shows difference maps between CMAQ and OMI in rural areas of the U.S. Since this was a first-pass analysis, to avoid the cumbersome task of applying census data to establish urban and rural regions, rural areas were designated in a simplistic way - by setting a concentration threshold in the OMI data that masked out urban emissions. In January, the threshold for rural designation was set at below 4 x 10^{15} molecules/cm^2, and in July it was set at below 2 x 10^{15} molecules/cm^2.

With urban areas masked out, we see that the WIFE2.0 and LADCO difference maps look even more similar in both months, suggesting that urban emissions estimates comprise the most important difference between the inventories, and that maintaining rural highway network structure does not have much of an effect. In January, both inventory model runs are too low in the Southwestern U.S., and still too high in rural parts of the upper Midwest. However, in the Northwest, and rural Southeast and northern New England, model-satellite differences are close to zero. In July, both inventory model runs are too low in virtually all rural areas of the U.S. One possible explanation for this difference may be the absence of accounting for NO_x emissions from lightning in both the LADCO nonfreight inventory, and the CMAQ model, which research suggests increases upper tropospheric ozone concentrations by 60-75% over the Eastern U.S. [41].

Next we examine model validation of the basecase 12 km x 12 km CMAQ model runs over the Midwestern U.S. The value of conducting a model and inventory validation

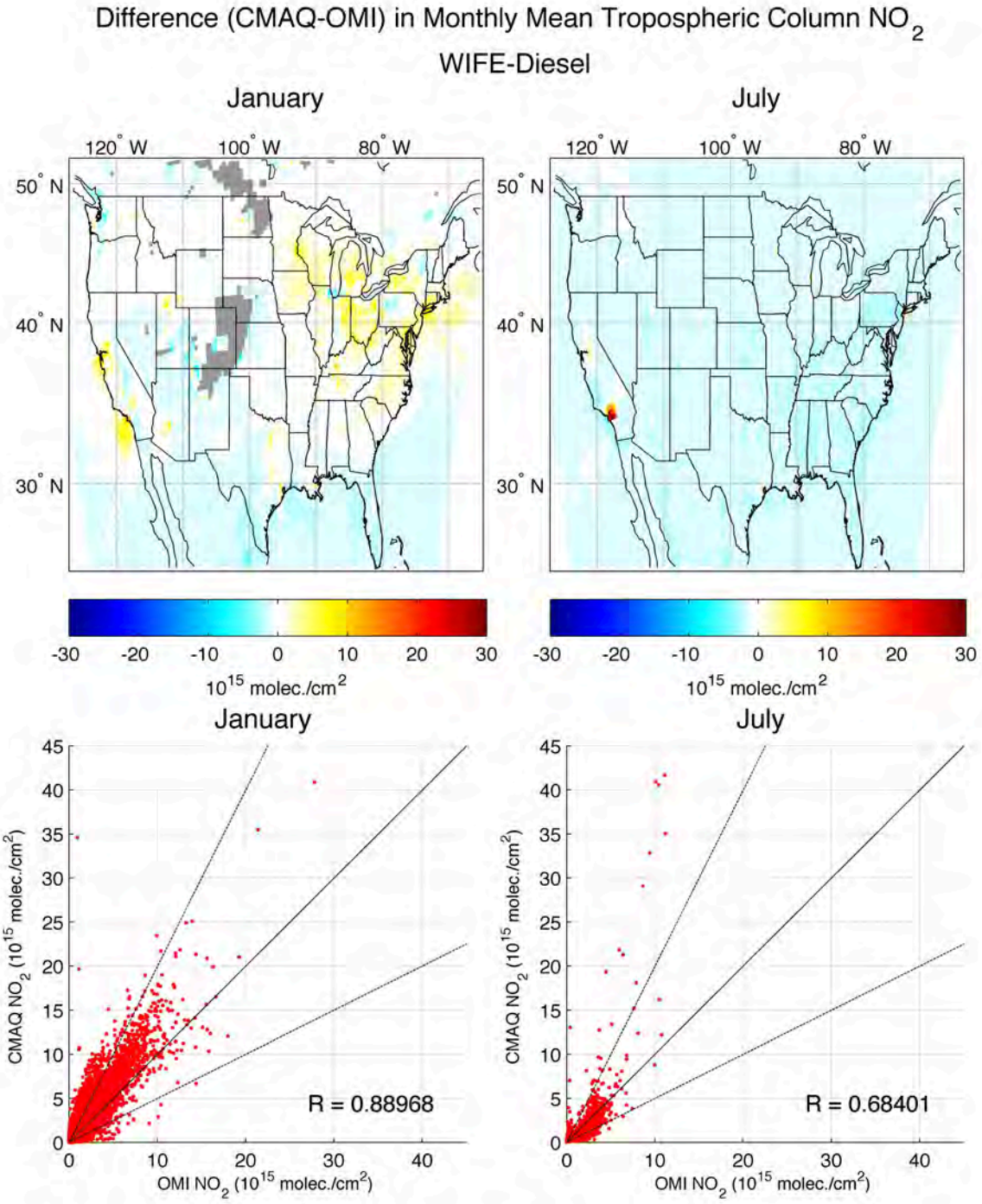

Figure 3.1.3 *Difference between 36 km x 36 km CMAQ modeled monthly mean tropospheric column NO_2 using the WIFE diesel inventory and monthly mean OMI tropospheric column NO2 for a) January and b) July 2007. CMAQ modeled c) January and d) July monthly mean tropospheric column NO2 (y-axis) scattered against monthly mean monthly mean OMI tropospheric column NO_2 (x-axis), with a 1:1 line (solid), a 2:1 line (dashed), and spatial correlation value, R.*

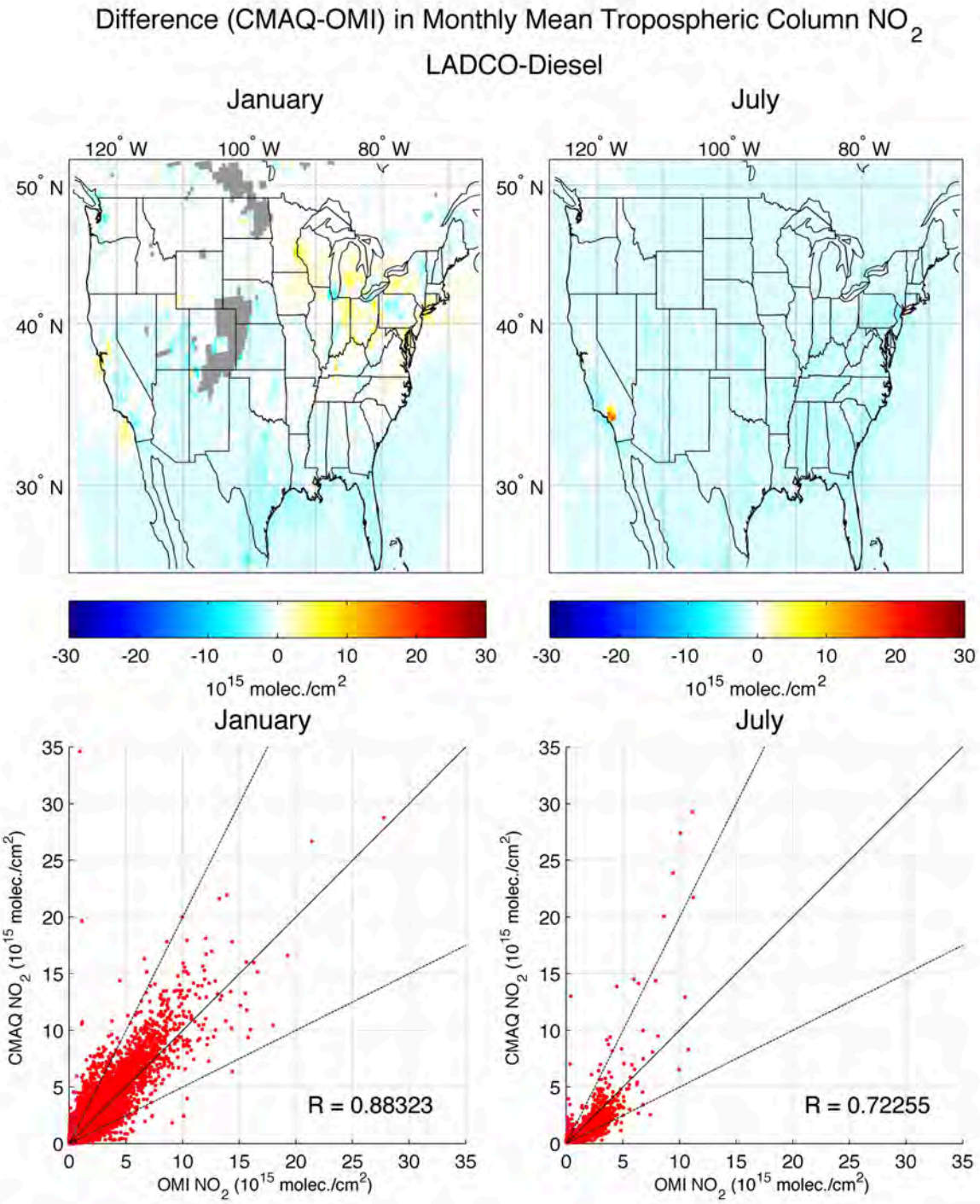

Figure 3.1.4 *Difference between 36 km x 36 km CMAQ modeled monthly mean tropospheric column NO_2 using the LADCO diesel inventory and monthly mean OMI tropospheric column NO2 for a) January and b) July 2007. CMAQ modeled c) January and d) July monthly mean tropospheric column NO2 (y-axis) scattered against monthly mean monthly mean OMI tropospheric column NO_2 (x-axis), with a 1:1 line (solid), a 2:1 line (dashed), and spatial correlation value, R.*

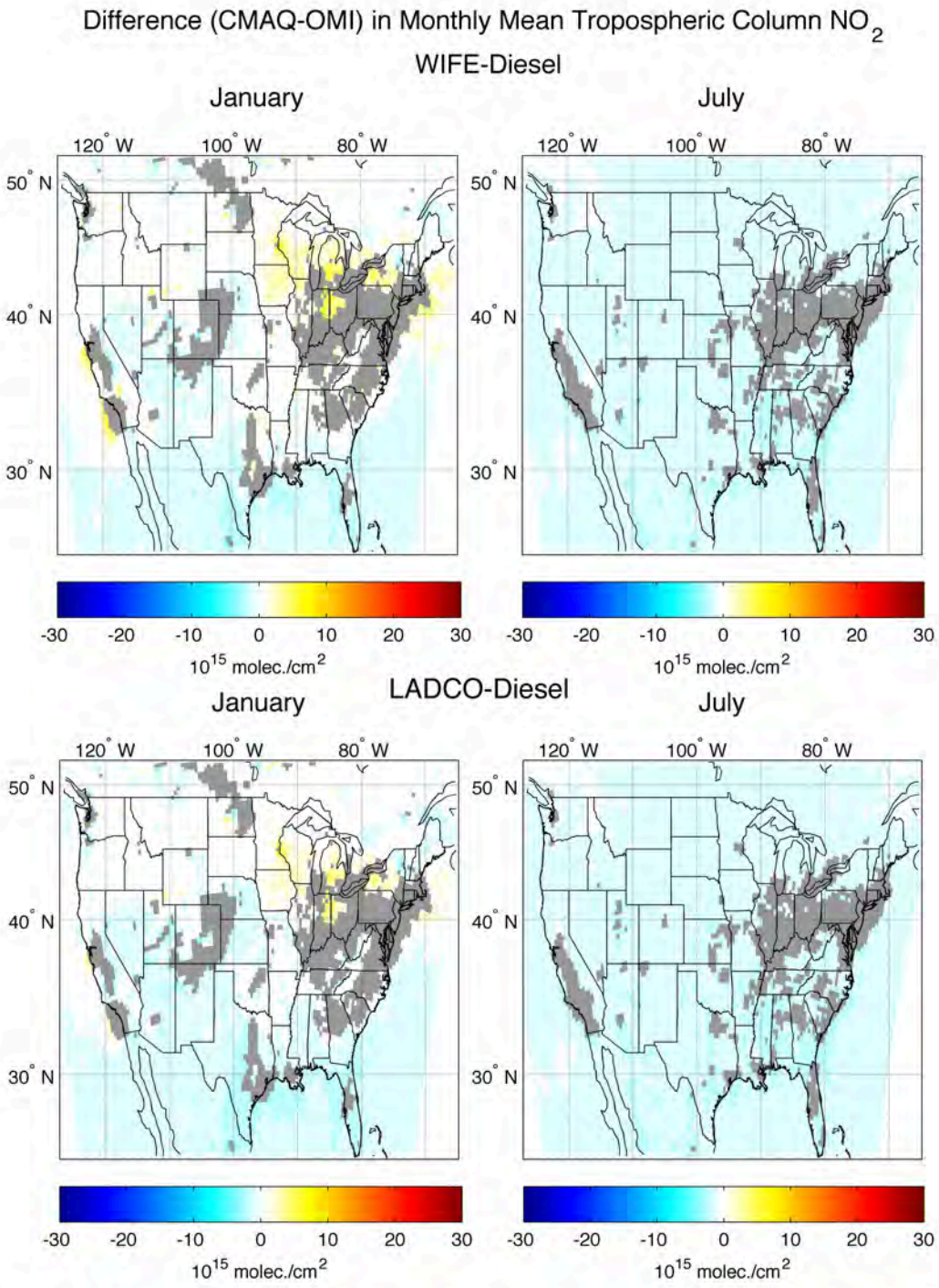

Figure 3.1.5 *Difference between 36 km x 36 km rural CMAQ modeled monthly mean tropospheric column NO_2 and rural monthly mean OMI tropospheric column NO_2 for a) January and b) July 2007 with the WIFE diesel inventory, and c) January and d) July 2007 with the LADCO diesel inventory. Rural areas were classified by concentration of OMI tropospheric NO_2 - 4 x 10^{15} molec./cm^2 for January, and 2 x 10^{15} molec./cm^2 for July.*

analysis over two spatial domains and model scales is to get a more detailed look at emissions sources in a region, and determine the role of scale in model performance relative to observations. Do the models and inventories perform better at a finer scale, suggesting we are estimating emissions profiles well from the start, or do larger scales washout variability at finer resolutions and therefore perform better?

Figures 3.1.6 and 3.1.7 show monthly mean surface NO_2 modeled for the Midwest with CMAQ using the WIFE2.0 and LADCO diesel emissions inventories, overlaid with, and scattered against monthly mean surface AQS NO_2 observations. Patterns and magnitudes of NO_2 concentrations are similar between the two model inventories, with emissions from roadway networks much more distinct in the WIFE2.0 model output. Modeled NO_2 concentrations are also slightly higher in rural areas in the WIFE2.0 inventory model run for both January and July. Modeled surface concentrations with both diesel inventories skew a bit lower than AQS observations for both January and July, with moderate correlation values around 0.54.

Figures 3.1.8 and 3.1.9 show difference maps between basecase 12 km x 12 km Midwest CMAQ modeled monthly mean tropospheric column NO_2 and OMI monthly mean tropospheric column NO_2 for the WIFE2.0 and LADCO diesel inventory model runs, and scatterplots of modeled column NO_2 against OMI column NO_2. In January, difference plots show elevated model emissions across most of the Midwest, except for Chicago and the plains states at the western edge of the domain. The most elevated emissions appear to be point-sources (power plants and industry) along the Ohio River Valley. Emissions for point sources came from the LADCO 2007 inventory and were the same for both basecase model runs. In addition, the WIFE2.0 inventory model run is more elevated than the LADCO diesel inventory model run in rural areas of Ohio, Indiana, Michigan, and Illinois. In the 12 km x 12 km maps for both basecase runs, we also see higher localized emissions just outside Chicago, and in central and southeastern Illinois as well as the western edge of Lake Erie, which were not visible in the 36 km x 36 km maps. In July, as was observed in the 36 km x 36 km national maps, modeled tropospheric column NO_2 concentrations are lower than satellite NO_2. The exception to this trend are the cities of Chicago, Minneapolis, Detroit, St. Louis and a few smaller urban areas, where both basecase model runs are too high. Interestingly, both basecase model runs seem to perform well in suburban areas in July, particularly around Minneapolis, Chicago and Detroit. These urban-scale results are largely washed out in the national 36 km x 36 km run, highlighting the utility of analysis at finer resolution.

Scatterplots of CMAQ and OMI tropospheric column NO_2 again show good agreement for both model runs. The performance of the WIFE2.0 inventory in July improves slightly from R=0.68 (36 km x 36 km) to R=0.75 (12 km x 12 km). For the 12 km x 12 km Midwest domain, January scatterplots for both model runs are clustered above the 1:1 line - as they were for the 36 km x 36 km national model run - with correlations around

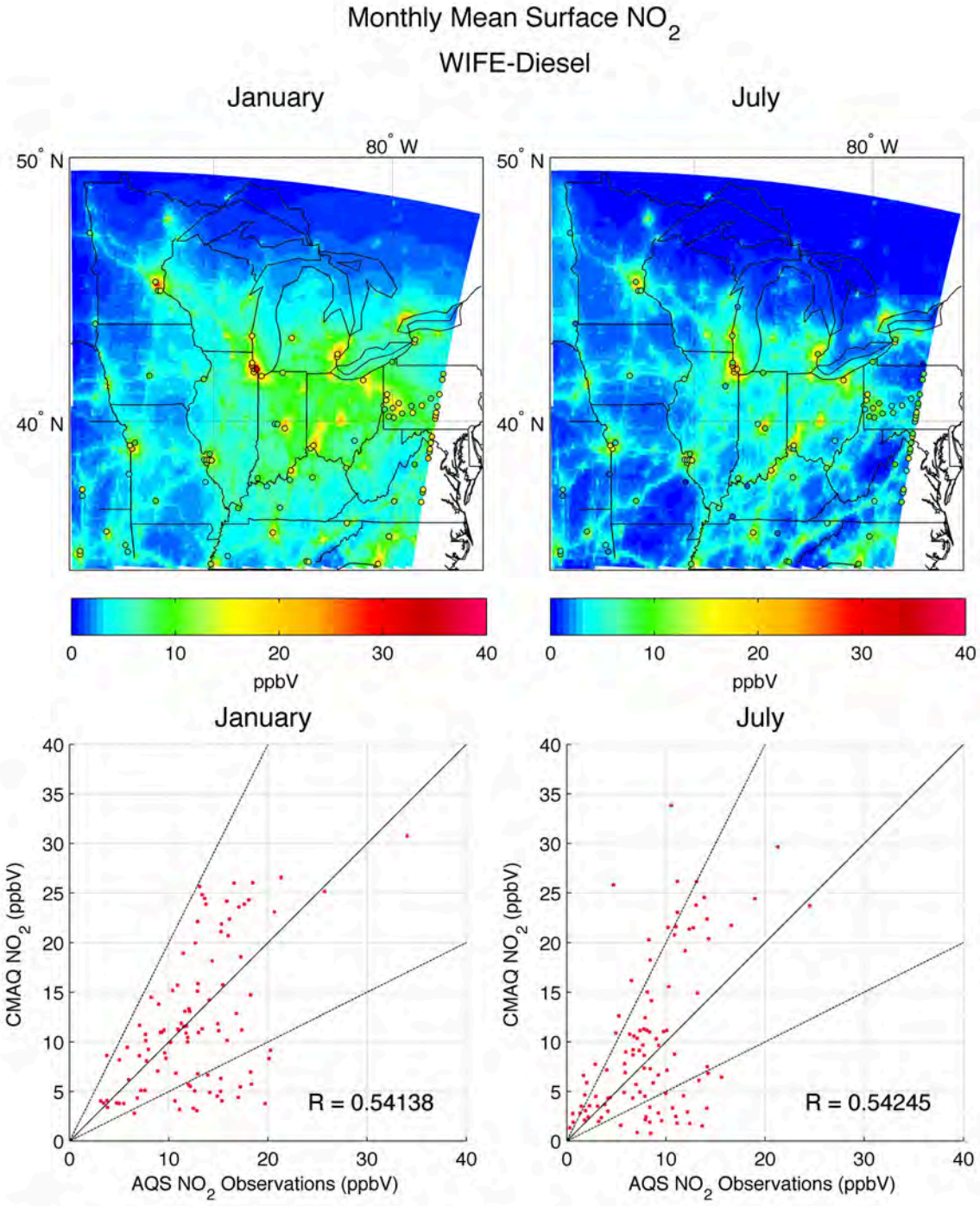

Figure 3.1.6 *CMAQ modeled 12 km x 12 km a) January and b) July 2007 monthly mean surface NO_2 using the WIFE diesel inventory, overlaid with monthly mean AQS NO2 observations. CMAQ modeled c) January and d) July monthly mean surface NO_2 (y-axis) scattered against monthly mean AQS observations (x-axis), with a 1:1 line (solid), a 2:1 line (dashed), a 1:2 line (dashed), and spatial correlation value, R.*

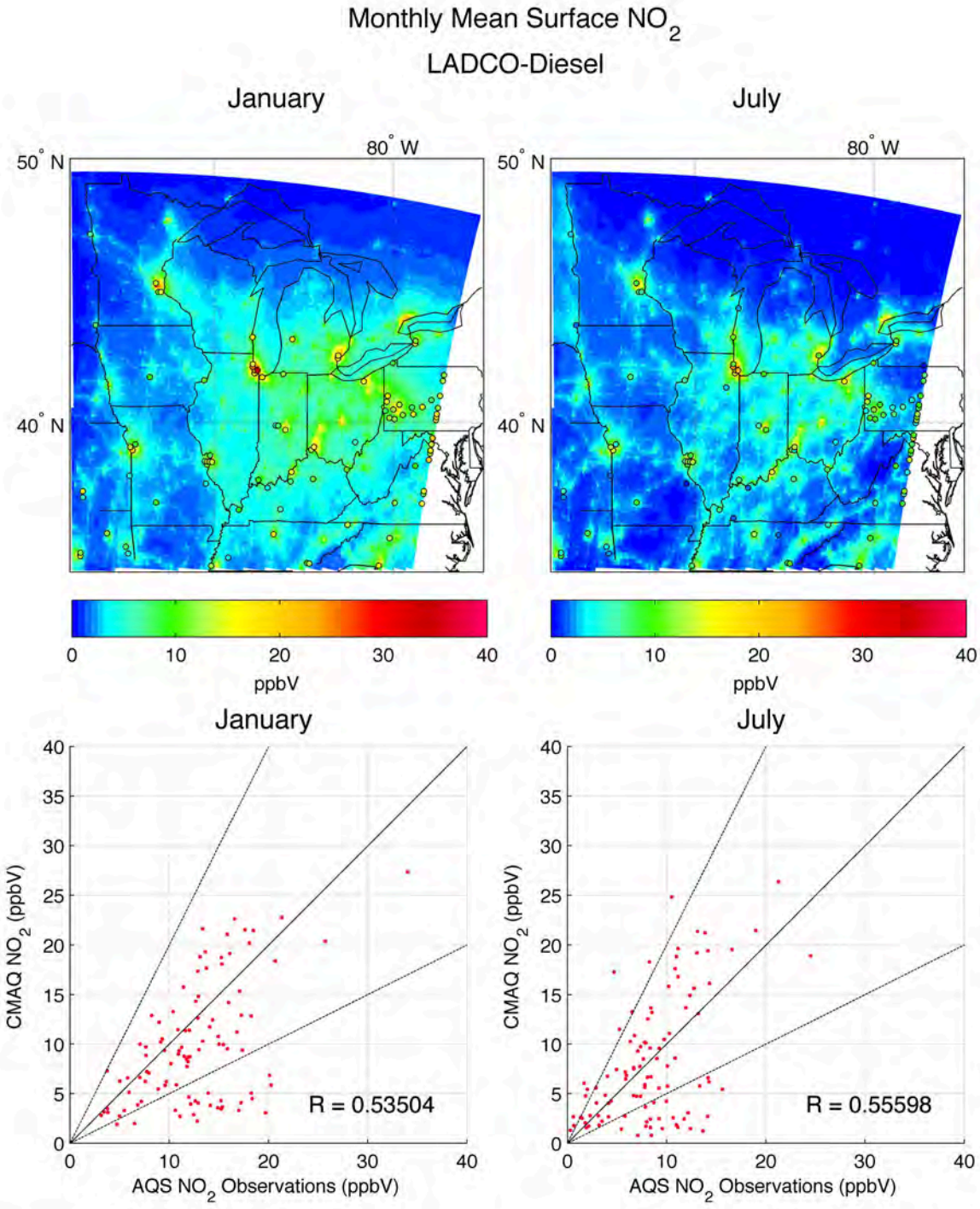

Figure 3.1.7 *CMAQ modeled 12 km x 12 km a) January and b) July 2007 monthly mean surface NO_2 with the LADCO diesel inventory, overlaid with monthly mean AQS NO2 observations. CMAQ modeled c) January and d) July monthly mean surface NO_2 (y-axis) scattered against monthly mean AQS observations (x-axis), with a 1:1 line (solid), a 2:1 line (dashed), a 1:2 line (dashed), and spatial correlation value, R.*

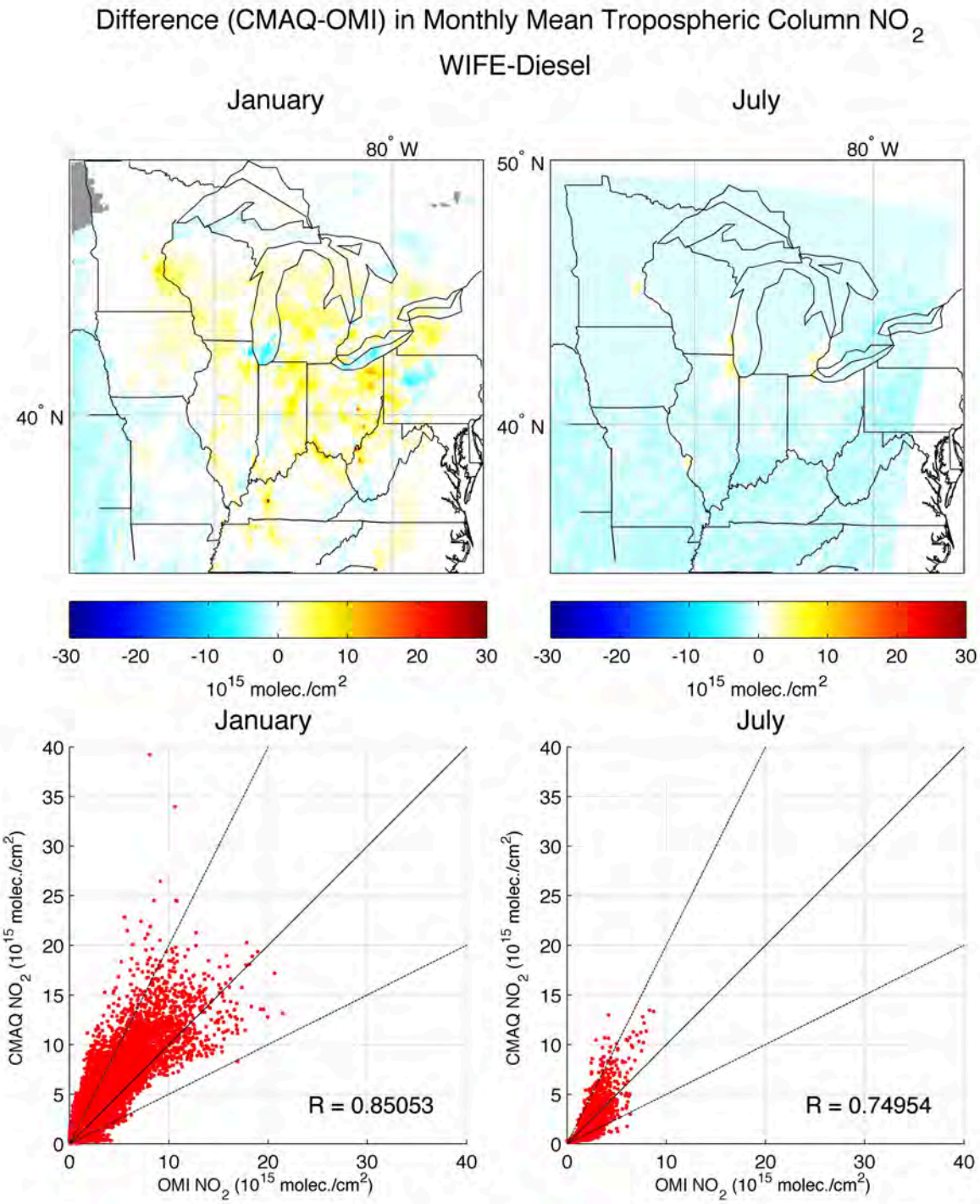

Figure 3.1.8 *Difference between 12 km x 12 km CMAQ modeled monthly mean tropospheric column NO_2 with the WIFE diesel inventory and monthly mean OMI tropospheric column NO2 for a) January and b) July 2007. CMAQ modeled c) January and d) July monthly mean tropospheric column NO2 (y-axis) scattered against monthly mean monthly mean OMI tropospheric column NO_2 (x-axis), with a 1:1 line (solid), a 2:1 line (dashed), and spatial correlation value, R.*

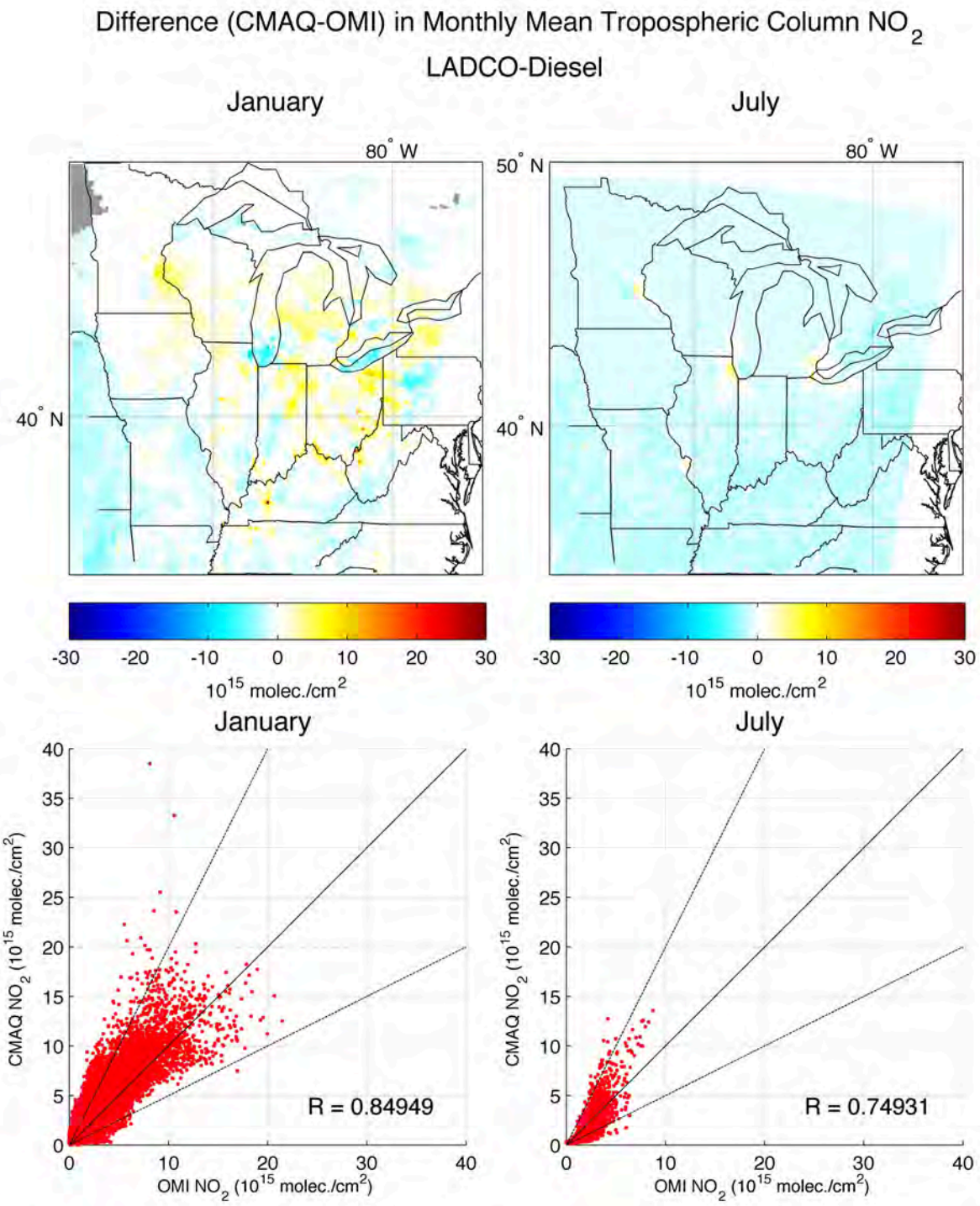

Figure 3.1.9 *Difference between 12 km x 12 km CMAQ modeled monthly mean tropospheric column NO_2 with the LADCO diesel inventory and monthly mean OMI tropospheric column NO2 for a) January and b) July 2007. CMAQ modeled c) January and d) July monthly mean tropospheric column NO2 (y-axis) scattered against monthly mean monthly mean OMI tropospheric column NO_2 (x-axis), with a 1:1 line (solid), a 2:1 line (dashed), and spatial correlation value, R.*

0.85, and July correlations around 0.75.

Summary statistics of CMAQ basecase model validation against AQS and OMI NO_2 for both domains are shown in Table 3.1.1. Included in the table are CMAQ model validation metrics described by Eder and Yu [42]; mean-r, where daily mean NO_2 values are correlated over time and averaged over space, normalized mean bias (NMB), and normalized mean error (NME). The number of spatial points for comparison is given by n, with monthly mean spatial correlation values (from the scatterplots), R. Additional to

CMAQ Model Scenario		CONUS 36 km x 36 km				MIDWEST 12 km x 12 km			
		LADCO Diesel		WIFE Diesel		LADCO Diesel		WIFE Diesel	
	Metric	January	July	January	July	January	July	January	July
AQS surface NO_2	mean-r	0.39	0.37	0.39	0.36	0.34	0.29	0.37	0.28
	NMB (%)	-35.5	-0.3	-14.5	25.9	-21.6	-4.1	-3.3	15.9
	NME (%)	49.5	49.6	45.8	62.4	45.5	56.6	47.4	67.0
	n	266	271	266	271	100	103	100	103
	R	0.60	0.65	0.64	0.67	0.54	0.56	0.54	0.54
OMI trop. column NO_2	mean-r	0.37	0.16	0.37	0.17	0.44	0.22	0.45	0.22
	NMB (%)	8.2	-41.3	30.6	-37.2	26.5	-41.4	44.1	-38.5
	NME (%)	74.3	62.7	84.2	62.7	73.4	61.0	82.1	60.3
	n	15,967	16,576	15,967	16,576	19,190	19,564	19,190	19,564
	R	0.88	0.72	0.89	0.68	0.85	0.75	0.85	0.75
OMI trop. column NO_2 at AQS gridcells	mean-r	0.53	0.25	0.53	0.25	0.34	0.20	0.35	0.22
	NMB (%)	11.6	4.2	37.0	29.5	14.2	1.8	30.1	9.4
	NME (%)	52.2	62.6	65.0	79.4	56.4	68.1	64.3	70.4
	n	265	271	265	271	99	103	99	103
	R	0.87	0.82	0.88	0.82	0.81	0.87	0.81	0.85
OMI trop. column NO_2 in rural areas	mean-r	0.65	0.16	0.35	0.16	0.45	0.24	0.46	0.24
	NMB (%)	6.7	-45.5	29.0	-43.2	41.9	-47.1	62.0	-44.9
	NME (%)	87.1	65.0	96.6	63.9	96.2	62.5	107.2	61.7
	n	14,596	15,233	14,596	15,233	13,467	14,080	13,467	14,080
	R	0.73	0.67	0.75	0.69	0.64	0.69	0.64	0.69

Table 3.1.1 *CMAQ model validation statistics compared to AQS surface NO_2 measurements and OMI tropospheric column NO_2 retrievals. Statistical metrics include mean-r, where daily values are correlated over time and averaged over space, Normalized Mean Bias (NMB), and Normalized Mean Error (NME). Mean-r, NMB and NME statistics use daily values (see Eder and Yu, 2006). For CMAQ-AQS comparisons, daily values are 24-hour means, for CMAQ-OMI comparisons, daily values are from the OMI overpass time. The monthly mean spatial points of comparison is represented by n, and R is the spatial correlation of monthly mean values (see scatterplots).*

the table are OMI validation statistics in gridcells with AQS monitors. Because AQS NO_2 monitors are generally located in and around urban areas, AQS validation statistics are more representative of urban model performance, whereas OMI validation statistics are more spatially comprehensive. To see whether AQS and OMI validation metrics agree, we validated CMAQ against OMI in gridcells containing AQS monitors. The table also includes CMAQ-OMI rural validation metrics for the 12 km x 12 km Midwest domain, for which the maps were not shown. Among all the model validation metrics, there is not a "clear winner" between the WIFE2.0 and LADCO diesel freight emissions inventories. The WIFE2.0 inventory often shows slightly better spatial correlation with observations (especially in January), but with higher bias and error - a possible indication that WIFE2.0 improves upon the spatial distribution of freight truck emissions, but not their magnitudes.

3.2 Surface NO_2 and Column NO_2

The principal motivation for using satellite retrieved pollutant metrics to inform ground-based transportation emissions inventories is the assumed relationship between tropospheric column NO_2 and surface NO_2. Here, we test that relationship in air quality model output. Figures 3.2.1 and 3.2.2 show maps of monthly mean surface NO_2, and monthly mean tropospheric column NO_2 for the 36 km x 36 km national domain, and the 12 km x 12 km Midwest domain. Surface NO_2 concentrations were processed to match the daily OMI retrieval time, and masked where satellite data did not exist. The relationship between surface and column NO_2 was quantified by taking the spatial correlation of the monthly means. For the 36 km x 36 km national domain, correlations were 0.84, and 0.87 for January and July, respectively. For the 12 km x 12 km Midwest domain, correlations were 0.63 and 0.69, for January and July, respectively. To investigate whether surface-column spatial correlation differences between the 36 km x 36 km domain and the 12 km x 12 km domain were the result of resolution or emissions in the domain, we also correlated 36 km x 36 km surface and column NO_2 concentrations constrained within the Midwest domain. Results showed spatial correlation values of 0.71 in January and 0.67 in July. The large discrepancy between model resolutions is likely due to more spatially concentrated emissions in the 12 km x 12 km model run compared to the 36 km x 36 km run.

The maps and results are for CMAQ basecase model runs with the WIFE2.0 diesel inventory. Because the relationship between surface and column NO_2 depends more on model transport and dispersion algorithms than emissions inputs, results for the basecase CMAQ run with the LADCO diesel inventory were very similar.

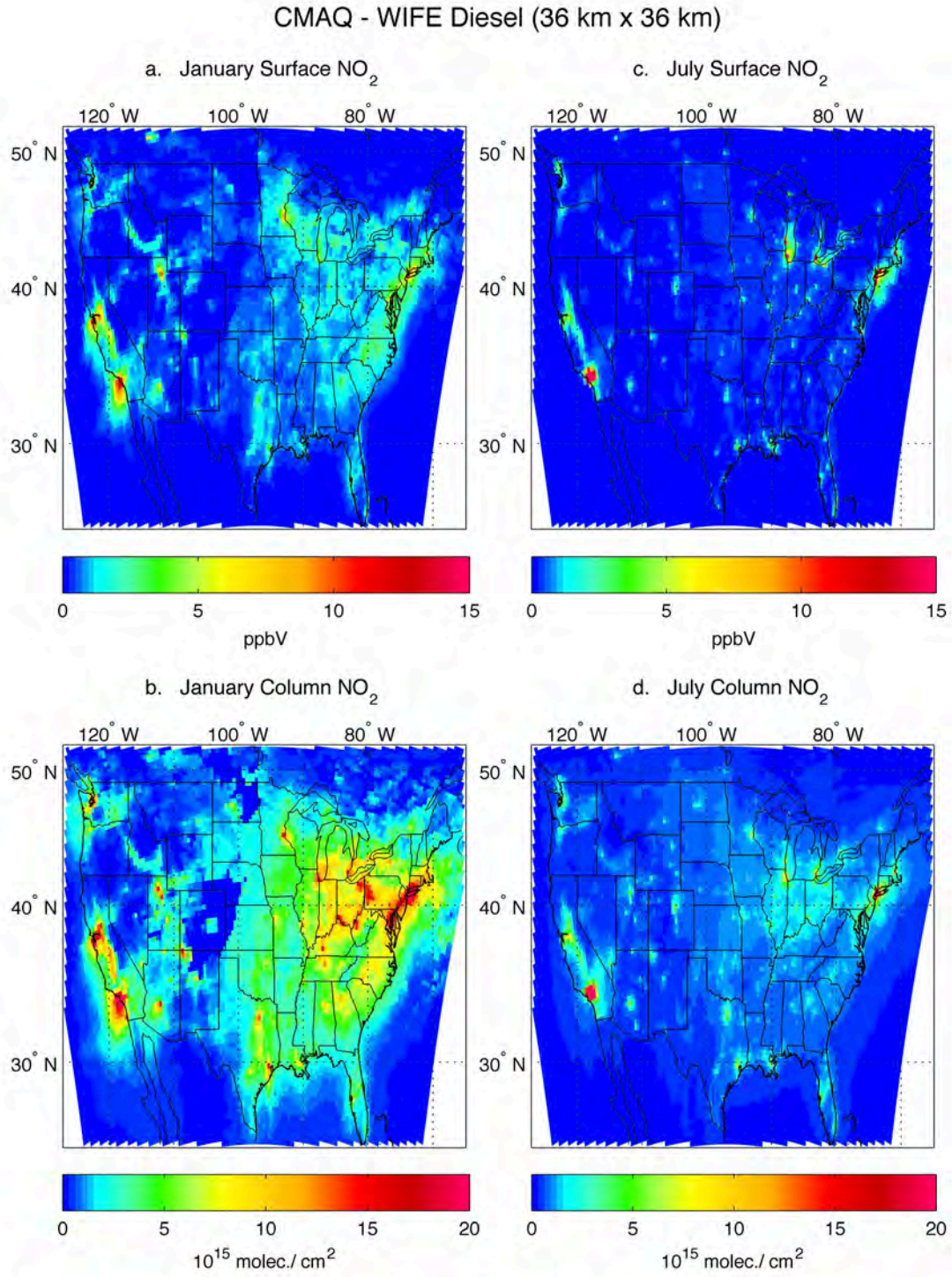

Figure 3.2.1 *CMAQ 36 km x 36 km monthly mean surface NO_2 for a) January and b) July 2007 with the WIFE diesel inventory, and CMAQ 36 km x 36 km monthly mean tropospheric column NO_2 for c) January and d) July 2007. The spatial correlation between surface and column NO_2 for January is 0.84, and for July is 0.87.*

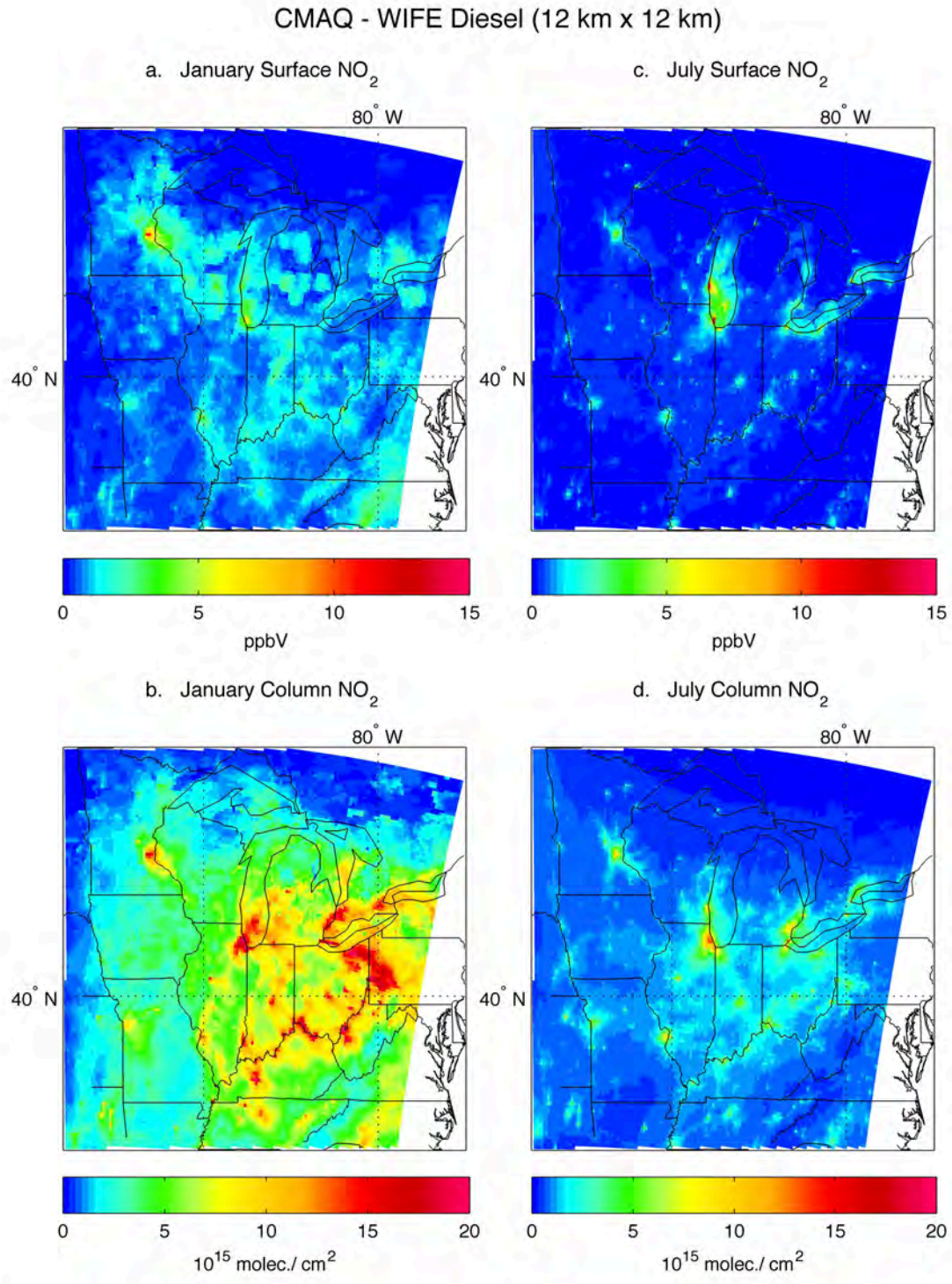

Figure 3.2.2 *CMAQ 12 km x 12 km monthly mean surface NO_2 for a) January and b) July 2007 with the WIFE diesel inventory, and CMAQ 12 km x 12 km monthly mean tropospheric column NO_2 for c) January and d) July 2007. The spatial correlation between surface and column NO_2 for January is 0.63, and for July is 0.69.*

3.3 Freight Pollution Attribution

Note: Results in this section are preliminary. An error in power plant emissions inputs was subsequently discovered that may affect quantitative results, however, qualitative results are presumed unaffected.

In maps of OMI tropospheric column NO_2 retrievals, where large populations and urban activity are absent, emissions primarily from transportation are readily evident. One such example in the Western U.S., is the region of southern Idaho, as well as in northeast Wyoming. While transportation related emissions in Wyoming are almost certainly due to heavy freight rail traffic traveling to and from coal mines in the region,

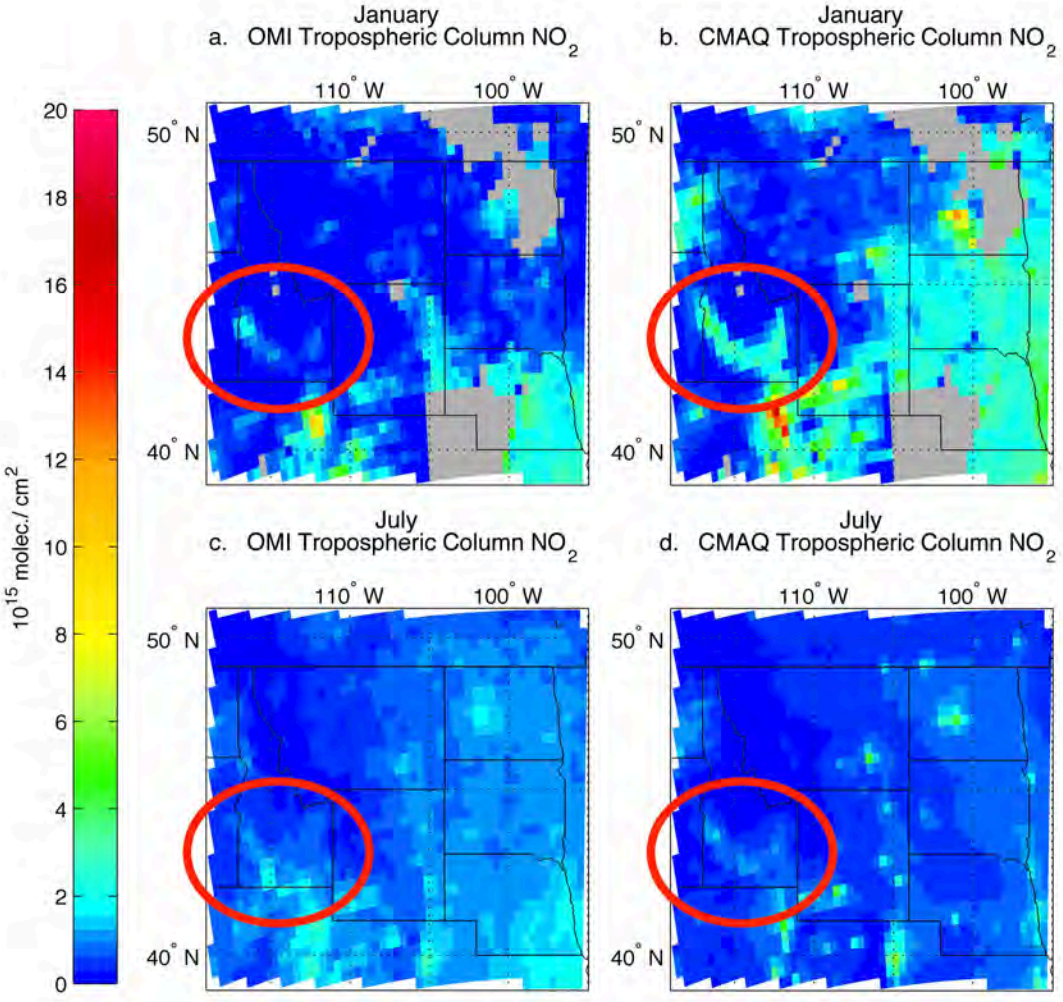

Figure 3.3.1 *Western U.S. OMI 36 km x 36 km monthly mean tropospheric column NO_2 for a) January and c) July, and CMAQ 36 km x 36 km monthly mean tropospheric column NO_2. Transportation NO_2 concentrations are visible in both OMI and CMAQ maps along highway and railway corridors in southern Idaho (circled in red), and near large coal mines in northeastern Wyoming.*

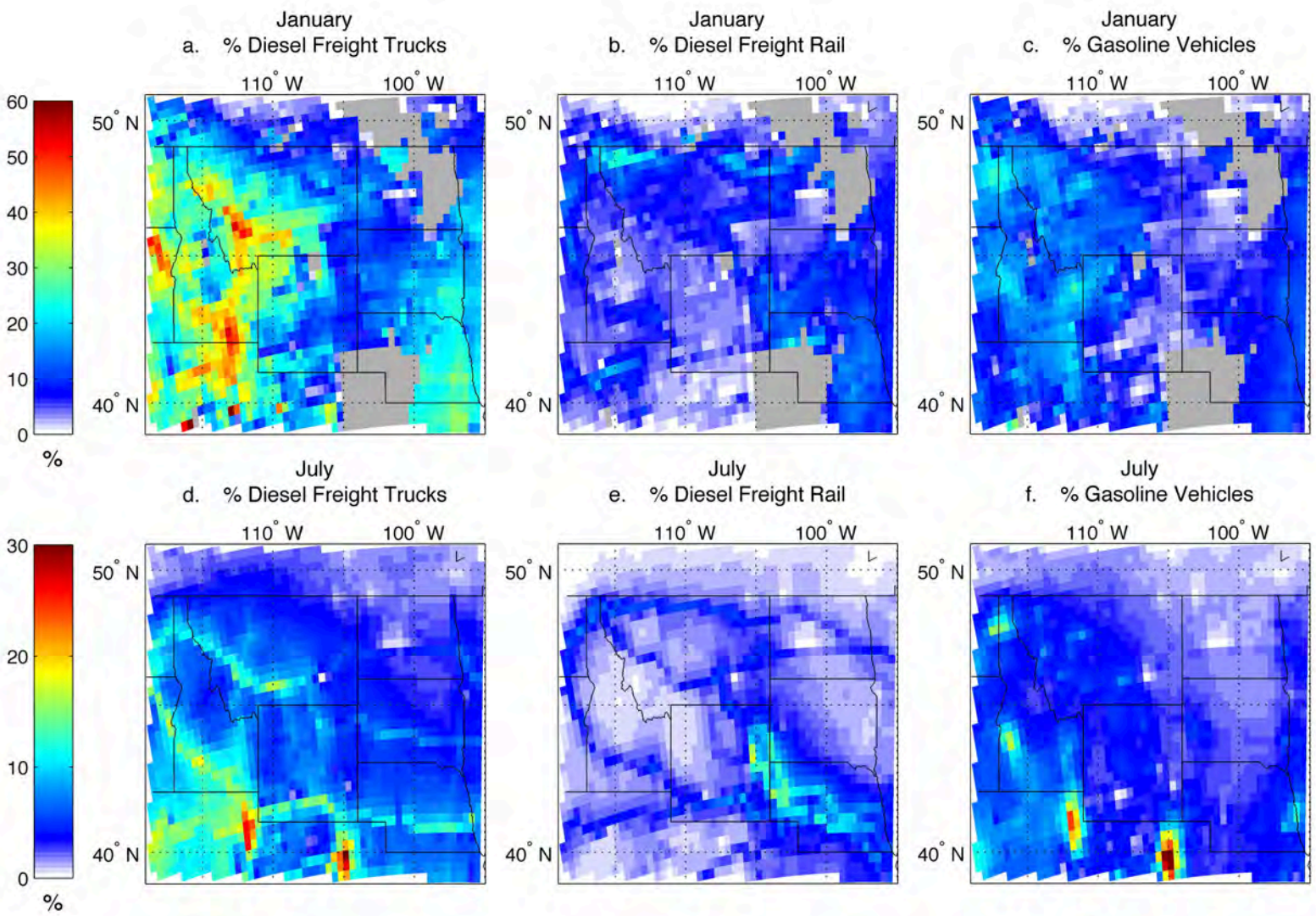

Figure 3.3.2 *Western U.S. 36 km x 36 km CMAQ % of monthly mean tropospheric column NO_2 from a) & d) diesel freight trucks, b) & e) diesel freight rail, and c) & f) gasoline vehicles for January and July 2007. Interstate 84 and a Union Pacific rail line run parallel in southern Idaho. Coal mines in eastern Wyoming are responsible for heavy freight rail traffic in that region.*

the primary sources in southern Idaho are more uncertain. Interstate-84 and a Union Pacific rail line run parallel to one another. To investigate the primary sources of these emissions seen in satellite retrievals, we use CMAQ experimental runs where transportation sectors were removed, compared to the basecase model runs to attribute pollution. Figure 3.3.1 shows maps of tropospheric column NO_2 from OMI and the WIFE2.0 CMAQ basecase run for January and July 2007. In all four maps, particularly in January in CMAQ, we see emissions along the southern Idaho corridor. In July, modeled NO_2 emissions are lower than OMI, though more understated roadway and railway network patterns are still evident.

Figure 3.3.2 shows tropospheric column NO_2 pollution attribution maps for the region for diesel freight trucks, diesel freight rail, and gasoline vehicles. In the model, the majority of January NO_2 emissions along the southern Idaho corridor are attributable to freight trucks at about 45%, with gasoline vehicles accounting for about 20% and rail activity 10%. In the northern part of the region, at the Canadian border, rail emissions comprise as much as 25% of NO_2. In July, diesel freight trucks dominate highways, while both gasoline vehicles and diesel trucks dominate urban areas (Boise, ID; Salt Lake City, UT; Denver, CO). Extensive freight rail activity is also visible around the coal mines of eastern Wyoming where the BNSF rail line operates. Here, freight rail accounts for up to 20% of NO_2 emissions.

4. Summary and Conclusions

In this analysis we built a new version of the bottom-up WIFE diesel truck freight emissions inventory for 2007, using FAF3 and the EPA MOVES model. WIFE2.0, improves upon previous WIFE versions by including emissions inventories for both freight and non-freight diesel vehicles, as well as accounting for idling and cold start emissions. We also employed the new ERTAC freight rail bottom-up emissions inventory in an air quality modeling analysis with the CMAQ model. Modeled emissions of NO_2 were validated against surface measurements and satellite NO_2 data. The performance of WIFE2.0 was compared to the 2007 LADCO diesel emissions inventory. Results showed somewhat better spatial correlation between model simulations with the WIFE2.0 diesel inventory, though higher levels of bias and error than the LADCO inventory. This suggests that while WIFE2.0 may improve on the spatial resolution of diesel freight truck emissions, emissions magnitudes need adjusting.

This analysis represents the first study to employ satellite data to evaluate surface freight transportation emissions. The value of satellite data is much higher spatial coverage with which to compare against model output, compared to existing surface monitor networks. This helps inform emissions trends outside urban areas where surface monitors often do not exist. Overall, satellite data offered a useful comparative

tool, with some limitations. One limitation is the absence of satellite data on cloudy days, or when surface reflectivity is high, for example due to snow cover. In monthly mean tropospheric column NO_2 for January 2007, there was a large area across the mountain west with no data for the entire month, and many areas across the U.S. with fewer than 15 days of data for the month. Another limitation is temporal resolution. Whereas surface monitors for NO_2 collect hourly measurements, NO_2 data from OMI, and other polar orbiting satellite instruments, is only available for one overpass time per day. These limitations highlight the importance of operating both satellite instruments, and surface monitors. One has high spatial resolution and low temporal resolution, while the other has low spatial resolution and high temporal resolution. Though a geostationary satellite instrument platform [43], could greatly improve temporal data resolution, it would not be expected to resolve cloud interference limiting data retrieval.

In this analysis, we also quantified the relationship between surface concentrations of NO_2, and tropospheric column NO_2 from the CMAQ model. Spatial correlations of monthly mean concentrations across the 36 km x 36 km national domain were high (0.84 and 0.87 for January and July, respectively), while spatial correlations for the 12 km x 12 km Midwest domain were quite a bit lower (0.63 and 0.69). The difference, as shown by evaluating 36 km x 36 km correlations over the Midwest domain (0.71 and 0.67) is due to inventory and model performance over the region - July correlation values are similar at both grid resolutions, and localized high concentrations in January increase variability in the 12 km x 12 km model run.
Finally, we examine pollution attribution of freight related emissions visible from OMI NO_2 retrievals over southern Idaho and eastern Wyoming. Though transportation network-like emissions activity was readily visible in the satellite data, because a highway and railway operate in parallel, it was unknown which freight mode was contributing to pollution more. By comparing CMAQ model runs with and without key transportation related emissions sources, we determined that according to the emissions inventories, diesel freight trucks were responsible for the majority of NO_2 emissions along that corridor, followed by gasoline vehicles and diesel locomotives.

Overall, this work highlights the utility of satellite data for both model validation and constraining emissions sources, especially in concert with ground-based monitors, with which surface and atmospheric column model performance can be compared. The wealth of data available from models, satellites, and monitors opens up a wide range of possible analysis directions for future work.

References

[1] U. S. EPA, "NO2: Health," *US Environmental Protection Agency*, Jul. 2011.

[2] U. S. EPA, "Ozone and Your Health," *US Environmental Protection Agency*, Feb-2009. [Online]. Available: http://www.epa.gov/airnow/ozone-c.pdf. [Accessed: 07-Jun-2012].

[3] G. J. Frost, S. A. Mckeen, M. Trainer, T. B. Ryerson, J. A. Neuman, J. M. Roberts, A. Swanson, J. S. Holloway, D. T. Sueper, T. Fortin, D. D. Parrish, F. C. Fehsenfeld, F. Flocke, S. E. Peckham, G. A. Grell, D. Kowal, J. Cartwright, N. Auerbach, and T. Habermann, "Effects of changing power plant NO xemissions on ozone in the eastern United States: Proof of concept," *J. Geophys. Res.*, vol. 111, no. 12, p. D12306, 2006.

[4] D. Mauzerall, B. Sultan, and N. Kim, "NOx emissions from large point sources: variability in ozone production, resulting health damages and economic costs," *Atmospheric Environment*, 2005.

[5] E. M. Perera, "Climate Change and Your health Rising Temperatures, Worsening Ozone Pollution," May 2011.

[6] K. Knowlton, J. Rosenthal, C. Hogrefe, B. Lynn, S. Gaffin, R. Goldberg, C. Rosenzweig, K. Civerolo, J. Ku, and P. Kinney, "Assessing ozone-related health impacts under a changing climate," *Environ Health Persp*, vol. 112, no. 15, pp. 1557–1563, 2004.

[7] U. S. EPA, "Air Emission Sources: Nitrogen Oxides," *United States Environmental Protection Agency*, pp. 1–2, Apr. 2012.

[8] AASHTO, "Unlocking Freight," American Association of State Highway and Transportation Officials, Jul. 2010.

[9] U. S. EIA, *Annual Energy Outlook 2011, With Projections to 2035*. U.S. Energy Information Administration, 2011.

[10] R. M. Hoff and S. A. Christopher, "Remote Sensing of Particulate Pollution from Space: Have We Reached the Promised Land?," *JAWMA*, vol. 59, no. 6, pp. 645–675, 2009.

[11] R. J. van der A, H. J. Eskes, F. Boersma, van Noije, T. P. C., M. van Roozendael, I. De Smedt, D. H. M. U. Peters, and E. W. Meijer, "Trends, seasonal variability and dominant NOx source derived from a ten year record of NO2 measured from space," *J Geophys Res-Atmos*, vol. 113, pp. –, 2008.

[12] S. Kim, A. Heckel, S. McKeen, G. Frost, E. Hsie, M. Trainer, A. Richter, J. Burrows, S. Peckham, and G. Grell, "Satellite-observed US power plant NOx emission reductions and their impact on air quality," *Geophys. Res. Lett.*, vol. 33, no. 5, p. L22812, 2006.

[13] A. R. Russell, L. C. Valin, E. J. Bucsela, M. O. Wenig, and R. C. Cohen, "Space-based Constraints on Spatial and Temporal Patterns of NOx Emissions in California, 2005-2008," *Environ. Sci. Technol.*, vol. 44, no. 9, pp. 3608–3615, 2010.

[14] A. Richter, V. Eyring, J. Burrows, H. Bovensmann, A. Lauer, B. Sierk, and P. Crutzen, "Satellite measurements of NO2 from international shipping emissions," *Geophys. Res. Lett.*, vol. 31, no. 23, pp. –, 2004.

[15] T. Marbach, S. Beirle, U. Platt, P. Hoor, F. Wittrock, A. Richter, M. Vrekoussis, M. Grzegorski, J. P. Burrows, and T. Wagner, "Satellite measurements of formaldehyde linked to shipping emissions," *Atmos. Chem. Phys.*, vol. 9, no. 21, pp. 8223–8234, 2009.

[16] E. Marmer, F. Dentener, J. von Aardenne, F. Cavalli, E. Vignati, K. Velchev, J. Hjorth, F. Boersma, G. Vinken, N. Mihalopoulos, and F. Raes, "What can we learn about ship emission inventories from measurements of air pollutants over the Mediterranean Sea?," *Atmos. Chem. Phys.*, vol. 9, no. 18, pp. 6815–6831, 2009.

[17] K. Franke, A. Richter, H. Bovensmann, V. Eyring, P. Joeckel, P. Hoor, and J. P. Burrows, "Ship emitted NO2 in the Indian Ocean: comparison of model results with satellite data," *Atmos. Chem. Phys.*, vol. 9, no. 19, pp. 7289–7301, 2009.

[18] M. de R. de Wildt, H. Eskes, and F. Boersma, "The global economic cycle and satellite-derived NO2 trends over shipping lanes," *Geophys. Res. Lett.*, vol. 39, pp. –, 2012.

[19] U. S. EPA, "Air Emissions Sources: Particulate Matter 2.5," *United States Environmental Protection Agency*, pp. 1–2, Apr. 2012.

[20] M. Johnston, E. Bickford, T. Holloway, C. Dresser, and T. M. Adams, "Impacts of biodiesel blending on

freight emissions in the Midwestern United States," *TRANSPORTATION RESEARCH PART D*, pp. 1–11, May 2012.
[21] E. Bickford and T. Holloway, "Sustainable Freight Infrastructure to Meet Climate and Air Quality Goals," *www.wistrans.org*, Feb-2012. [Online]. Available: http://www.wistrans.org/cfire/documents/FR_CFIRE0209.pdf. [Accessed: 27-May-2013].
[22] ORNL, "FAF3 Freight Traffic Analysis," *faf.ornl.gov*, 23-Mar-2011. [Online]. Available: http://faf.ornl.gov/fafweb/Data/Freight_Traffic_Analysis/faf_fta.pdf. [Accessed: 25-May-2013].
[23] S. Vallamsundar and J. Lin, "Overview of US EPA New Generation Emission Model: MOVES," *Proceedings of International Conference on Advances in Civil Engineering*, 2010.
[24] U. S. EPA, "Motor Vehicle Emission Simulator (MOVES)," *US Environmental Protection Agency*, Mar-2012. [Online]. Available: http://www.epa.gov/otaq/models/moves/documents/420b12001.pdf. [Accessed: 07-Jun-2012].
[25] SEMCOG, "Appendix C: On-Road Mobile Source Emissions Inventory for Southeast Michigan PM2.5 Redesignation Request," *michigan.gov*, 27-Jan-2011. [Online]. Available: http://www.michigan.gov/documents/deq/deq-aqd-Appendix-C-On-Road-Mobile-EM-Inv-PM25-Redes-Request_351255_7.pdf. [Accessed: 25-May-2013].
[26] A. S. Khan, N. N. Clark, G. J. Thompson, W. S. Wayne, M. Gautam, D. W. Lyon, and D. Hawelti, "Idle emissions from heavy-duty diesel vehicles: Review and recent data," *J Air Waste Manag Assoc*, vol. 56, no. 10, pp. 1404–1419, 2006.
[27] R. L. McCormick, M. S. Graboski, T. L. Alleman, and J. Yanowitz, "Idle emissions from heavy-duty diesel and natural gas vehicles at high altitude," *JAWMA*, vol. 50, no. 11, pp. 1992–1998, 2011.
[28] M. Houyoux, J. Vukovich, C. Coats, N. Wheeler, and P. Kasibhatla, "Emission inventory development and processing for the Seasonal Model for Regional Air Quality (SMRAQ) project," *J Geophys Res-Atmos*, vol. 105, pp. 9079–9090, 2000.
[29] M. Bergin, M. Harrell, J. McDill, M. Janssen, L. Driver, R. Fronczak, R. Nath, and D. Seep, "ERTAC Rail: A Collaborative Effort in Building a Railroad-Related Emissions Inventory between Eastern States' Air Protection Agencies and Participation with ...," *ERTAC*, 2009.
[30] M. Bergin, M. Harrell, and M. Janssen, "Rail Emissions Inventory Part 1: Class I Line-Haul Locomotives," Appendix A in Documentation for Locomotive Component of the National Emissions Inventory Methodology, 2011.
[31] M. Bergin, M. Harrell, and M. Janssen, "Rail Emissions Inventory Part 2: Class I Railyard Switcher Locomotives," Appendix C in Documentation for Locomotive Component of the National Emissions Inventory Methodology, 2011.
[32] M. Bergin, M. Harrell, and M. Janssen, "Rail Emissions Inventory Part 3: Class II and III Locomotives," Appendix B in Documentation for Locomotive Component of the National Emissions Inventory Methodology, 2011.
[33] D. Byun and K. L. Schere, "Review of the Governing Equations, Computational Algorithms, and Other Components of the Models-3 Community Multiscale Air Quality (CMAQ) Modeling System," *Appl. Mech. Rev.*, vol. 59, no. 2, p. 51, 2006.
[34] P. F. Levelt, G. H. J. van den Oord, M. R. Dobber, A. Malkki, H. Visser, J. de Vries, P. Stammes, J. O. V. Lundell, and H. Saari, "The ozone monitoring instrument," *IEEE Trans. Geosci. Remote Sensing*, vol. 44, no. 5, pp. 1093–1101, 2006.
[35] F. L. Herron-Thorpe, B. K. Lamb, G. H. Mount, and J. K. Vaughan, "Evaluation of a regional air quality forecast model for tropospheric NO2 columns using the OMI/Aura satellite tropospheric NO2 product," *Atmos. Chem. Phys.*, vol. 10, no. 18, pp. 8839–8854, 2010.
[36] F. Boersma, H. J. Eskes, R. J. Dirksen, R. J. van der A, J. P. Veefkind, P. Stammes, V. Huijnen, Q. L. Kleipool, M. Sneep, J. Claas, J. Leitão, A. Richter, Y. Zhou, and D. Brunner, "An improved tropospheric NO2 column retrieval algorithm for the Ozone Monitoring Instrument," *Atmos. Meas. Tech.*, vol. 4, no. 9, pp. 1905–1928, 2011.
[37] F. Boersma, F. Braak, and R. J. van der A, "Dutch OMI NO2 (DOMINO) data product v2.0," *temis.nl*. [Online]. Available: http://www.temis.nl/docs/OMI_NO2_HE5_2.0_2011.pdf. [Accessed: 18-Jan-2012].
[38] J. C. Hains, F. Boersma, M. Kroon, R. J. Dirksen, R. C. Cohen, A. E. Perring, E. Bucsela, H. Volten, D. P. J. Swart, and A. Richter, "Testing and improving OMI DOMINO tropospheric NO2 using observations from the DANDELIONS and INTEX-B validation campaigns," *J. Geophys. Res.*, vol.

115, p. D05301, 2010.
[39] M. N. Deeter, "Calculation and Application of MOPITT Averaging Kernels," *acd.ucar.edu*, 01-Jul-2002. [Online]. Available: http://www.acd.ucar.edu. [Accessed: 25-May-2013].
[40] H. J. Eskes and F. Boersma, "Averaging kernels for DOAS totalcolumn satellite retrievals," *Atmos. Chem. Phys.*, vol. 3, no. 5, pp. 1285–1291, 2003.
[41] D. J. Allen, K. E. Pickering, R. W. Pinder, B. H. Henderson, K. W. Appel, and A. Prados, "Impact of lightning-NO on eastern United States photochemistry during the summer of 2006 as determined using the CMAQ model," *Atmos. Chem. Phys.*, vol. 12, no. 4, pp. 1737–1758, 2012.
[42] B. Eder and S. Yu, "A performance evaluation of the 2004 release of Models-3 CMAQ," presented at the Atmospheric Environment, 2006, vol. 40, no. 26, pp. 4811–4824.
[43] W. A. Lahoz, V.-H. Peuch, J. Orphal, J. L. Attie, K. Chance, X. Liu, D. Edwards, H. Elbern, J. M. Flaud, M. Claeyman, and L. El Amraoui, "MONITORING AIR QUALITY FROM SPACE The Case for the Geostationary Platform," *Bull. Amer. Meteor. Soc.*, vol. 93, no. 2, pp. 221–233, 2012.
[44] MassGIS, "Trains ArcMap Layer File," *Massachusetts Office of Geographic Information (MassGIS)*, pp. 1–4, 2008.

Appendix I: Map of NO_2 Ground Monitors

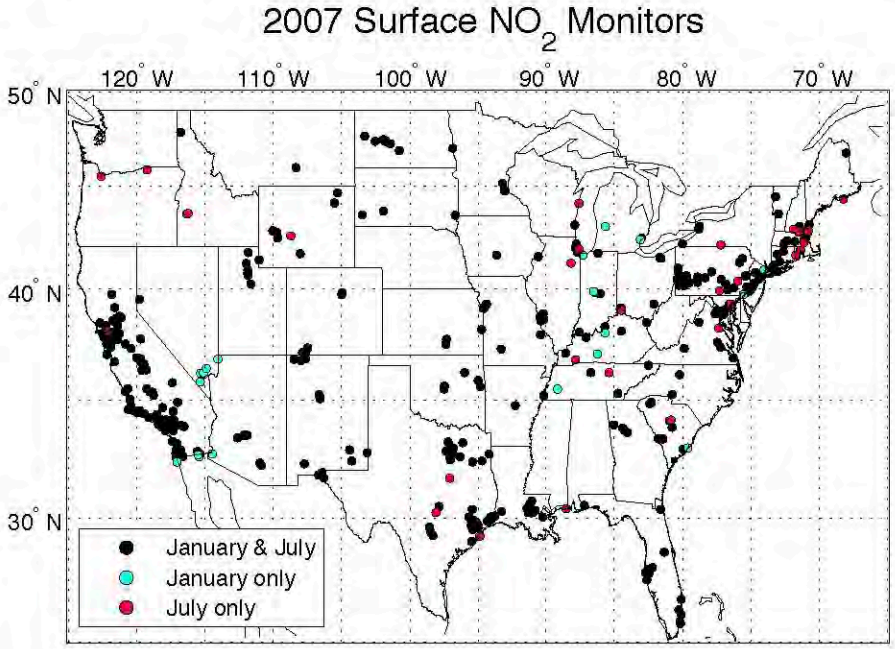

Figure I.i *Map of 2007 surface NO_2 monitor locations from EPA's AQS DataMart. Most monitor locations are in operation year-round, while others operate in winter or summer only.*

Appendix III: Documentation for Gridding ERTAC RAIL Inventories for Photochemical Modeling

Documentation for gridding the ERTAC rail emissions inventories onto a regional modeling grid, prepared by Erica Bickford for LADCO, January 2012.

This documentation details the methods used to grid the Eastern Regional Technical Advisory Committee's (ERTAC) 2007/2008 rail emissions inventory [30]-[32] to the Lake Michigan Air Directors Consortium's (LADCO) 4km x 4km national photochemical model grid.

III.i LADCO National 4km x 4km Inventory Grid

ERTAC 2007/2008 rail emissions for railyards, Class I rail and Class II & III rail were gridded to the LADCO 4km x 4km national grid (hereafter referred to as "LADCO 4km grid"), with the following specifications:
1983 North American Datum
Lambert Conformal Conic Projection
Central Meridian: -97
Latitude of Origin: 40
Standard Parallel 1: 33
Standard Parallel 2: 45
Lower Left Corner at -2628, -1980 km
Grid dimensions: 1,323 x 999 at 4km x 4km
At the Lower Left Corner: i-cell=1, j-cell=1

This LADCO 4km grid was created as a polygon shapefile in ArcGIS using a "fishnet" plug-in tool.

III.ii Class I Railyards

ERTAC Railyard emissions data was provided by LADCO (Mark Janssen) in excel spreadsheet form (filename: "ERTAC Railyard switcher emissions inventory public 11_2011.xls"), with each Railyard identified by latitude and longitude (representing the centroid of railyard polylines in GIS). Also provided was a shapefile of Railyards (filename: "fra_rail100k_yards_all.shp"). However, while there were 1,102 yards listed in the emissions table, there were 4,976 features in the rail shapefile. This is due to some Railyards being comprised of more than one rail segment. Also, in some cases multi-segment yards were identified as separate yards, for example with east and west components. This added a degree of complexity in matching emissions for each yard to its shapefile feature.

To grid Railyard emissions, the tabled emissions first needed to be spatially mapped in ArcGIS by joining emissions from the excel table to a yard shapefile. Rather than use the provided yard shapefile consisting of polylines, the latitude and longitude identifiers provided in the excel Railyard emissions table was imported into ArcGIS to create a point-shapefile, with the result that there was one shapefile feature corresponding to each Railyard in the emissions table (see Figure III.ii.i).

Emissions were joined to the Railyards as points, and by intersecting the emissions joined point-shapefile with the LADCO 4km grid polygon shapefile, each yard was assigned to a gridcell (by i-cell and j-cell). Using MS Access, emissions in the intersected emissions-joined grid shapefile database table were summed over each gridcell for each pollutant, and added to an empty LADCO 4km grid table.

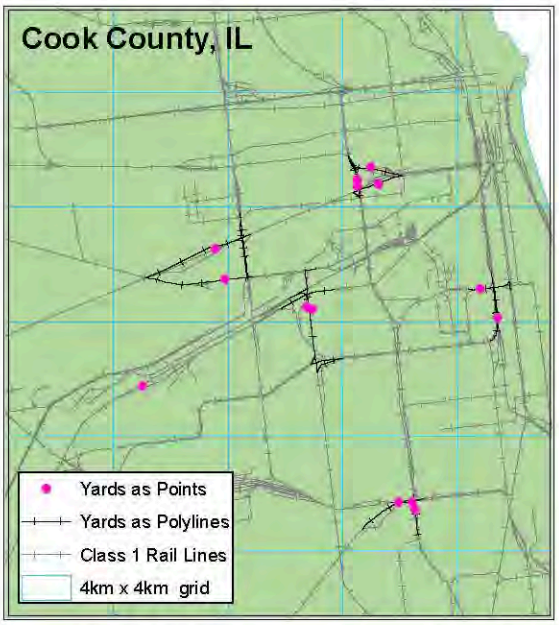

Figure III.ii.i Class 1 railyards in Cook County, IL as polylines (black hatched lines) from rail line segments, and points (pink dots) created from latitudes and longitudes.

III.iii Class I Line-haul

ERTAC Class I rail emissions data was provided by LADCO (Mark Janssen) in a MS Access database (filename: "Class1_Linehaul_Emissions_ Round6.mdb") with state and county emissions summary data provided in an excel spreadsheet (filename: "ERTAC Class 1 Line-Haul Inventory 11_2011.xls"). Within the MS Access database were several tables for Class I emissions factors, Class I emissions fleet mix emissions tiers, rail line owner, and queries relating them. Following guidance provided in "Access Queries.txt" (distributed with the Class I data files), a sequence of queries were used to generate a spatially-keyed table containing Class I emissions totals per rail link (using FRAARCID), per pollutant, and per primary owner (BNSF, CSX, UP, etc). The generated table did not include VOCs or CO_2, which were included in the summary Class I rail excel tables. Following ERTAC inventory, and EPA locomotive emissions documentation, VOC's were calculated from HC's using the formula:

$$VOCs = HC \times 1.053$$

Emissions of CO_2 were similarly calculated from CO, using the formula:

$$CO_2 = \text{CO} \times \frac{1.015 \times 10^4 \text{ grams/gal}}{26.624 \text{ grams/gal}}$$

Where 1.015x10^4 grams/gal is the diesel locomotive emissions factor for CO_2 given in the ERTAC Class I rail inventory documentation, and 26.624 grams/gal is the emissions factor for CO in the same documentation.

Emissions in the MS Access generated spatially linked table were organized by rail link, pollutant and line owner. Prior to gridding rail emissions, line owner information was removed by summing emissions over rail links (FRAARCID) by pollutant, and the Class I rail emissions table was reorganized such that pollution values were converted from row-data to column-data, with one row for each rail segment (identified by FRAARCID), and one column for each of the 9 pollutants.

In ArcGIS, the Class I rail polyline shapefile (filename: "FRA_rail100k_lines.shp") was mapped and intersected with the LADCO 4km grid polygon. Prior to intersecting the shapefile with the LADCO 4km grid polygon, rail segment miles were re-calculated using the ArcGIS "calculate geometry" feature. Although miles were included in the provided Class I shapefile, that shapefile was created using the 1984 North American Datum, whereas the LADCO grid is based on the 1983 North American Datum and projected to the Lambert Conformal Conic projection. Intersecting the 4km grid with the rail segment shapefile has the effect of splitting rail segments where they intersect grid boundaries, and applying the 4km grid shapefile's attributes, such as i-cell and j-cell, to each of the rail shapefile's features. Thus, emissions can be applied to the rail segment shapefile using FRAARCIDs, and then summed over grid indices. However, to avoid double-counting emissions, pollutant totals associated with the original rail segment lengths must be distributed to the new, intersected rail segment lengths using the ratio of the new length to the original length. To accurately compare the segment length ratios, it was necessary that the lengths both be calculated in the same way, under the same geographic and projected coordinate systems. After the Class I shapefile was intersected with the LADCO 4km grid, a new field was added to the shapefile attribute table, and the new, intersected rail segment lengths were calculated, also using "calculate geometry."

The intersected Class I shapefile was exported to an MS Access database table. Fields were created for each pollutant to hold original segment pollutant emissions, and a second set of fields was created to hold new segment-weighted emissions. Records for the original segment pollutant emissions fields were filled by matching FRAARCIDs between the Class I intersected shapefile, and the ERTAC Class I emissions table. Emissions for each new intersected rail segment were calculated by multiplying emissions of pollutant (p) per original rail segment (s) by the ratio of lengths in miles between the intersected rail segment (s_i) and the original rail segment (s).

$$EmisNew_{p,s_i} = EmisOrig_{p,s} \times \frac{MilesNew_{s_i}}{MilesOrig_s}$$

Where,
$EmisNew_{p,s_i}$ is the weighted emissions for pollutant p on the intersected partial rail segment, s_i
$EmisOrig_{p,s}$ is the emissions for pollutant p on the original rail segment, s
$MilesNew_{s_i}$ is the length (in miles) of the intersected partial rail segment, s_i
$MilesOrig_s$ is the length (in miles) of the original full rail segment, s

and, $\sum_{i=1}^{n} MilesNew_{s_i} = MilesOrig_s$

The newly calculated, weighted emissions were summed over each gridcell for each pollutant, and added to an empty LADCO 4km grid table.

Note here that Class I pollutant emission totals summed from the gridded inventory deviate slightly (about -0.00015%) from the reported totals in the ERTAC excel spreadsheet (see table 4-I.i). This is due to numerical precision loss exporting the rail shapefile from ArcGIS.

III.iv Class II & III Rail

ERTAC Class II & III (grouped together) emissions data was provided by LADCO (Mark Janssen) in MS Excel spreadsheet form (filename: "ERTAC Rail-Class II_III 10_2011.xls"). Emissions totals were given per county (STCNTYFIPS) and rail operator (Rep_Mark, for Reporting Marks – a rail operator abbreviation code). Without emissions spatially keyed to rail segments (eg. using FRAARCID, as with Class I rail), there were two options for gridding Class II & III emissions. 1.) Sum all emissions to the county level, and distribute to the 4km grid using the proportional area of each gridcell overlapping the county area. This method is relatively simple, however could induce significant error by dampening emissions across a larger area than they actually occur, particularly where counties are large. Option 2.) Link emissions to the Class II & III shapefile using county codes, operator codes, and emissions per track-mile factors back calculated from each county-operator emissions total. While this method possibly unreasonably assumes emissions for a given operator in a given county are evenly distributed along that operator's track, it does attribute emissions at the track-level, rather than the county-level. This documentation describes the methods used in for the latter method (option 2), which was employed to grid the Class II & III ERTAC emissions.

Starting with the Class II & III rail ArcGIS shapefile (filename: "class23_final_no-mgt.shp"), rail full-segment lengths were calculated in ArcGIS using the "calculate geometry" tool. Then, the shapefile was intersected with the LADCO 4km grid, and the intersected segment lengths were calculated in a new field.

The database table associated with the shapefile - including the full-segment, and intersected segment lengths - and the ERTAC Class II & III county–REP_MARK emissions table were imported into MS Access. The Excel table contained 2,652 rows of county code–operator code pairs. Of those, 2,591 rows contained non-zero emissions, representing 27,385 rail segment links. The GIS shapefile, however contained 24,411 links. The discrepancy is due to multiple operator use of some track segments. Since ERTAC emissions were calculated per county and operator, for each county-operator pair, there is a separate record. If two operators in the same county operate on the same track, then those track links will be listed twice, once for each operator. In order to match the shapefile links to the ERTAC emissions table, records from the shapefile database table were extracted by selecting for STCNTYFIPS and RROWNER/ TKRIGHTS (all fields) pairs matching STCNTYFIPS and REP_MARK pairs in the ERTAC emissions spreadsheet. Selecting this way allowed rail segments to be selected more than once, and after summing over operator-county codes, the number of records (representing county-operator pairs) was then 2,591 – the same as in the ERTAC Excel file.

To assign emissions to each rail segment without double-counting, county-operator emissions totals for each of the 9 pollutants needed to be converted to an emissions factor in tons per track mile. Then, the factor could simply be multiplied against the track miles for each intersected segment. Emission factors were calculated by dividing the total emissions of each pollutant per county-operator pair by the total number of miles operated on in the county by that operator. Here, the full segment track mile totals were used to ensure they matched the county-operator track mile totals listed in the ERTAC summary table. Then, the emissions per track mile factors were multiplied against the intersected segment miles. Emissions were then summed over grid cells (using the i-cell and j-cell attributes acquired from intersecting the rail shapefile with the LADCO 4km grid shapefile), and added to an empty LADCO 4km grid table.

Note here that similar to Class I rail, Class II & III pollutant emission totals summed from the gridded inventory deviate slightly (about -0.00049%) from the reported totals in the ERTAC excel spreadsheet (see table 4-I.ii). This again, is due to numerical precision loss exporting the rail shapefile from ArcGIS.

III.v Massachusetts Class II & III Scenic Emissions

For Class II & III rail, there was a special case in the ERTAC county-operator summary emissions table where an operator was listed with emissions and a county, but no track miles. The operators were "BSCR Berkshire" and "CCCR Cape Cod." These are both scenic rail lines operating in Massachusetts; the Berkshire Scenic Railway Museum (BSCR) operates in Berkshire County in western Massachusetts, and the Cape Cod

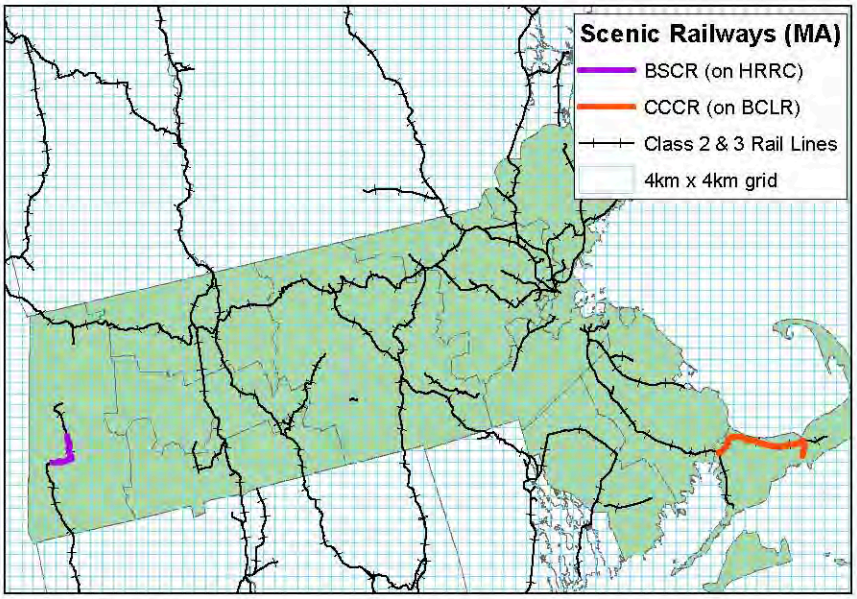

Figure III.ii Massachusetts scenic railways.

Central Railroad (CCCR) operates in Barnstable County on Cape Cod. Emissions for both of these operators were provided by the railroads, and added to the ERTAC inventory by the Massachusetts Department of Environmental Protection. However, within the provided Class II & III shapefile, no record of these operators existed in any of the RROWNER, TKRIGHTS, or PSNGR shapefile attribute fields. Therefore we were left to either apply the emissions to the entire county in which they operate, or track down another shapefile for them. Fortunately, a Google search turned up a result from the Massachusetts Office of Geographic Information for a Massachusetts specific rail shapefile that included the BSCR and CCCR in its attributes [44] (http://www.mass.gov/mgis/trains.htm). From that rail shapefile, it was found that the BSCR operates on several track segments of the HRRC - Housatonic Railroad Company Incorporated, and the CCCR operates on several track segments of the BCLR – Bay Colony Railroad (see Figure III.ii). Emissions totals for each scenic operator were distributed along the segments of track in which they run and added to the emissions of the freight operators on those segments.

The one caveat is that both of these scenic rail lines only operate in the summer. However since the ERTAC rail inventory does not currently include seasonality, summer emissions from these lines will be distributed throughout the year along with the freight operators, dampening pollutant concentrations during summer, when many of the severest air pollution episodes occur. The ERTAC inventory rail documentation has called for monthly or seasonal variation to be incorporated into future rail inventories, which will allow for scenic and other seasonal rail line emission to be more accurately accounted for.

III.vi Gridded File Formats

The final gridded files for the ERTAC 2007/2008 rail inventory are provided in the form of MS Access database tables, and .csv textfiles. The files are formatted in columns (see Figure III.iii), following the order:

stid (text): state FIPS code
ctid (text): county FIPS code
jcell (double): row cell index
icell (double): column cell index
CO, HC, VOC, NH3, NOx, PM2_5, PM10, SO2, CO2 (double): annual pollutant totals per grid cell

ERTAC_4kmgrid_class1.txt

```
"stid","ctid","icell","icell","CO","HC","VOC","NH3","NOx","PM2_5","PM10","SO2","CO2"
"0","0",161.00,1.00,0.00,0.00,0.00,0.00,0.00,0.00,0.00,0.00,0.00,0.00
"0","0",162.00,1.00,0.00,0.00,0.00,0.00,0.00,0.00,0.00,0.00,0.00,0.00
"0","0",163.00,1.00,0.00,0.00,0.00,0.00,0.00,0.00,0.00,0.00,0.00,0.00
"0","0",164.00,1.00,0.00,0.00,0.00,0.00,0.00,0.00,0.00,0.00,0.00,0.00
"0","0",165.00,1.00,0.00,0.00,0.00,0.00,0.00,0.00,0.00,0.00,0.00,0.00
"0","0",166.00,1.00,0.00,0.00,0.00,0.00,0.00,0.00,0.00,0.00,0.00,0.00
"0","0",167.00,1.00,0.00,0.00,0.00,0.00,0.00,0.00,0.00,0.00,0.00,0.00
"0","0",168.00,1.00,0.00,0.00,0.00,0.00,0.00,0.00,0.00,0.00,0.00,0.00
"0","0",169.00,1.00,0.00,0.00,0.00,0.00,0.00,0.00,0.00,0.00,0.00,0.00
"0","0",170.00,1.00,0.00,0.00,0.00,0.00,0.00,0.00,0.00,0.00,0.00,0.00
"0","0",171.00,1.00,0.00,0.00,0.00,0.00,0.00,0.00,0.00,0.00,0.00,0.00
"0","0",172.00,1.00,0.00,0.00,0.00,0.00,0.00,0.00,0.00,0.00,0.00,0.00
"0","0",173.00,1.00,0.00,0.00,0.00,0.00,0.00,0.00,0.00,0.00,0.00,0.00
"0","0",174.00,1.00,0.00,0.00,0.00,0.00,0.00,0.00,0.00,0.00,0.00,0.00
"0","0",175.00,1.00,0.00,0.00,0.00,0.00,0.00,0.00,0.00,0.00,0.00,0.00
"0","0",176.00,1.00,0.00,0.00,0.00,0.00,0.00,0.00,0.00,0.00,0.00,0.00
"0","0",177.00,1.00,0.00,0.00,0.00,0.00,0.00,0.00,0.00,0.00,0.00,0.00
"0","0",178.00,1.00,0.00,0.00,0.00,0.00,0.00,0.00,0.00,0.00,0.00,0.00
"0","0",179.00,1.00,0.00,0.00,0.00,0.00,0.00,0.00,0.00,0.00,0.00,0.00
"0","0",180.00,1.00,0.00,0.00,0.00,0.00,0.00,0.00,0.00,0.00,0.00,0.00
"0","0",181.00,1.00,0.00,0.00,0.00,0.00,0.00,0.00,0.00,0.00,0.00,0.00
"0","0",182.00,1.00,0.00,0.00,0.00,0.00,0.00,0.00,0.00,0.00,0.00,0.00
"0","0",183.00,1.00,0.00,0.00,0.00,0.00,0.00,0.00,0.00,0.00,0.00,0.00
"0","0",184.00,1.00,0.00,0.00,0.00,0.00,0.00,0.00,0.00,0.00,0.00,0.00
"0","0",185.00,1.00,0.00,0.00,0.00,0.00,0.00,0.00,0.00,0.00,0.00,0.00
"0","0",186.00,1.00,0.00,0.00,0.00,0.00,0.00,0.00,0.00,0.00,0.00,0.00
"0","0",187.00,1.00,0.00,0.00,0.00,0.00,0.00,0.00,0.00,0.00,0.00,0.00
"0","0",188.00,1.00,0.00,0.00,0.00,0.00,0.00,0.00,0.00,0.00,0.00,0.00
"0","0",189.00,1.00,0.00,0.00,0.00,0.00,0.00,0.00,0.00,0.00,0.00,0.00
```

Figure III.iii Gridded emissions csv file format.

The first row of the textfile contains the text headers for each column. Note that stid and ctid are only given for general spatial information purposes. A 4km x 4km grid cell can overlap two or more states and counties, with only one combination reported here. Grid cells outside of the U.S. contain "0" for both stid and ctid.

Figures III.iv to III-iv show examples of gridded NOx emissions for railyards, Class-I, and Class-II/III rail (plotted in Matlab from .csv files).

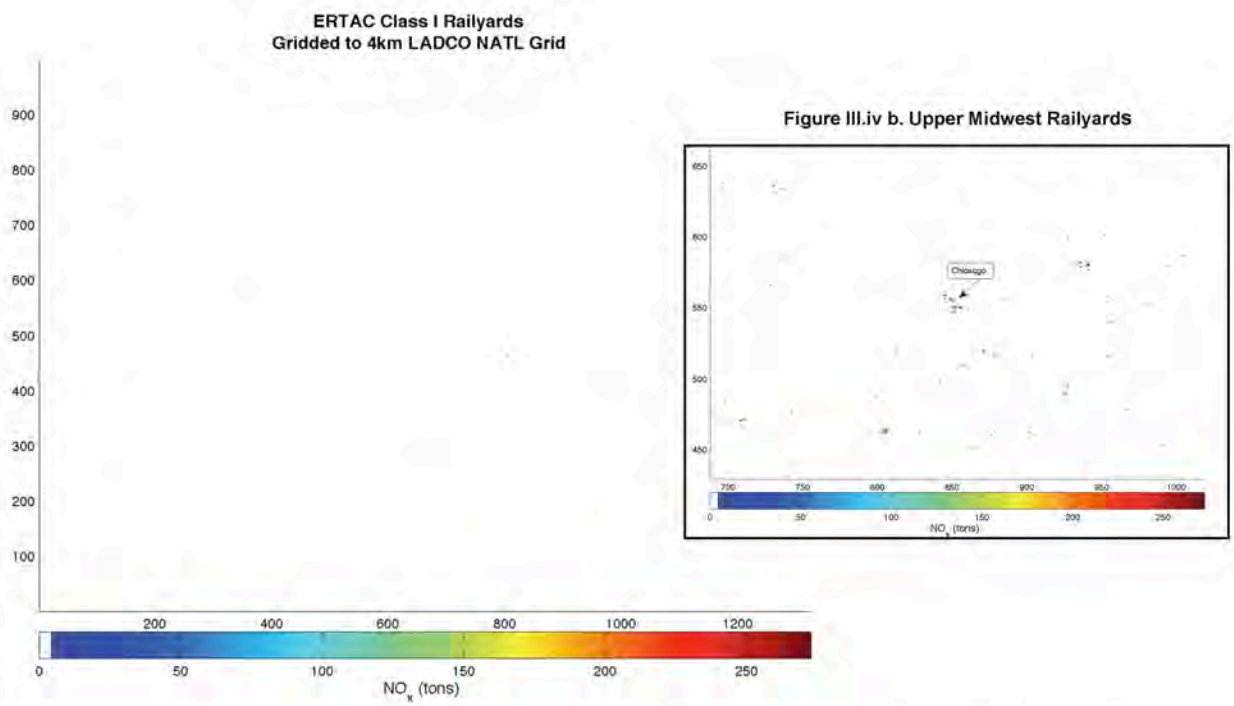

Figures III.iv a and b Gridded ERTAC Railyard emissions. At 1,323 x 999 grid resolution, the 4km x 4km gridded railyard points are very small and not easily visible. The inset, Figure 4-I.iv b. is a zoom-in of railyards in the upper Midwest, with Chicago at the center. Note the actual data maximum is 1,361 tons, but the color bar was scaled in an effort to make data points more visible.

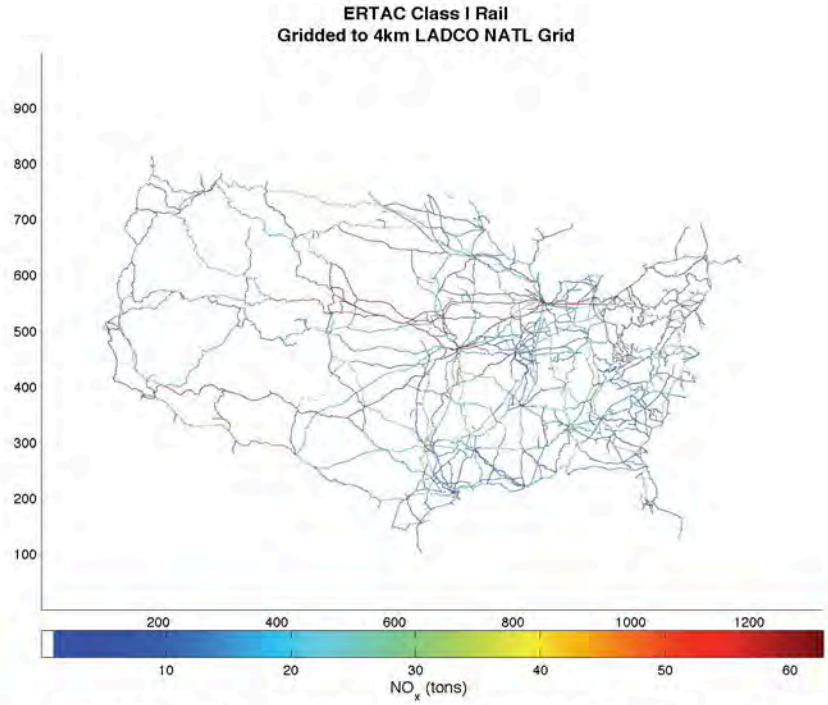

Figure III.v Gridded ERTAC Class I rail emissions. Actual maximum = 313 tons, colorbar scaled to highlight the entire network.

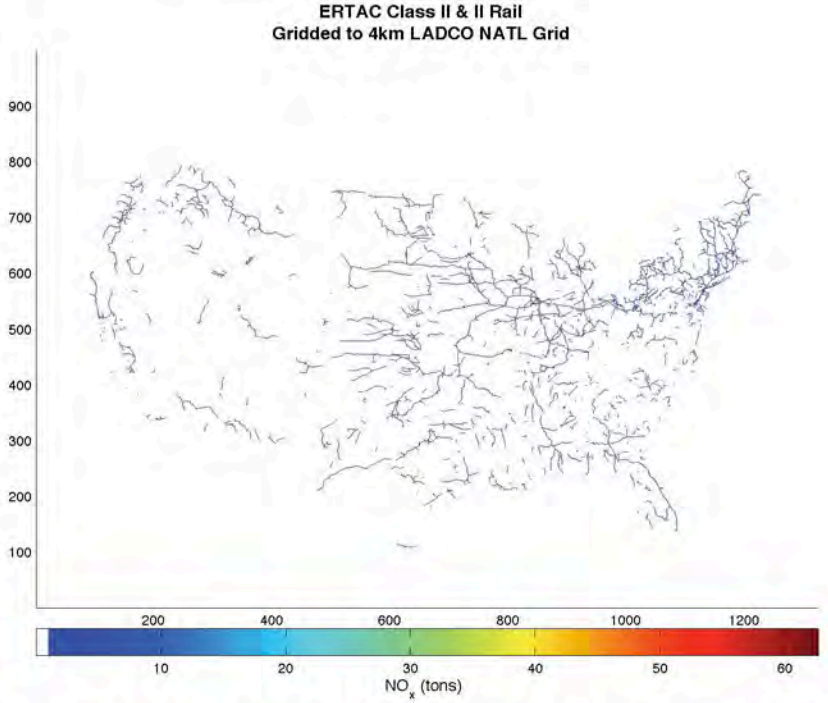

Figure III.vi Gridded ERTAC Class II & III rail emissions. Actual maximum = 47 tons, this colorbar was scaled to match the Class I map.

III.vii Emissions Summary Comparisons

After the ERTAC Class I and Class II & III rail emissions inventories were gridded to the LADCO 4km x 4km national grid, pollutant emissions were re-totaled and found to deviate slightly from the national pollutant summary totals distributed with the original ERTAC data. The differences were on the order of -0.00015% for Class I rail (see Table III.i), and -0.00049% for Class II & III (see Table III.ii), and result from data precision loss (decimal truncation) in the rail segment mile measurements when exporting the rail network shapefiles from ArcGIS to MS Access. This caused the sum of intersected rail segment lengths to not quite equal the original rail segment lengths. The issue was researched further, and is apparently consistent with other user experience when exporting shapefile attribute tables from ArcGIS to database programs. Since the difference was small, and not easily overcome, no further effort was made to correct it. Because Railyards were joined to emissions at points, no track mile calculations were made, and therefore gridded Railyard emissions totals match ERTAC summary tables.

Table III.i

Pollutant (Tons)	Tabled ERTAC Class I National Summary	Gridded ERTAC Class I National Summary	% Difference
CO	110,968.6456	110,968.4825	-0.00015%
HC	37,940.7049	37,940.6496	-0.00015%
VOC	N/A	39,951.5041	N/A
NH3	347.1937	347.1932	-0.00015%
NOx	754,433.1926	754,432.0772	-0.00015%
PM10	25,477.4163	25,477.3792	-0.00015%
PM2.5	23,439.2230	23,439.1888	-0.00015%
SO2	7,835.8282	7,835.8167	-0.00015%
CO2	42,305,136.5263	42,305,066.7683	-0.00016%

Table III.ii

Pollutant (Tons)	Tabled ERTAC Class II & III National Summary	Gridded ERTAC Class II & III National Summary	% Difference
CO	4,631.1057	4,631.0830	-0.00049%
HC	1,736.6617	1,736.6531	-0.00049%
VOC	1,828.7047	1,828.6958	-0.00049%
NOX	47,034.6500	47,034.4193	-0.00049%
PM10	1,157.7823	1,157.7767	-0.00049%
PM25	1,065.1541	1,065.1488	-0.00049%
NH3	14.4887	14.4887	-0.00049%
SO2	327.0056	327.0040	-0.00049%
CO2	1,764,993.2461	1,764,984.5917	-0.00049%

CFIRE

University of Wisconsin-Madison
Department of Civil and Environmental Engineering
1410 Engineering Drive, Room 270
Madison, WI 53706
Phone: 608-263-3175
Fax: 608-263-2512
cfire.wistrans.org